Microbiome

RESEARCH

Open Access

Rumen microbiome associates with postpartum ketosis development in dairy cows: a prospective nested case–control study

Fanlin Kong[1†], Shuo Wang[1†], Yijia Zhang[2], Chen Li[3], Dongwen Dai[4], Cheng Guo[4], Yajing Wang[1], Zhijun Cao[1], Hongjian Yang[1], Yanliang Bi[5], Wei Wang[1] and Shengli Li[1*]

Abstract

Background Approximately, one-third of dairy cows suffer from postpartum diseases. Ketosis is considered an important inducer of other postpartum diseases by disrupting energy metabolism. Although the rumen microbiome may be involved in the etiology of ketosis by supplying volatile fatty acids, the rumen environmental dynamics of ketosis cows are unclear. Using multi-omics, this study aimed to elucidate changes in the rumen microbiome during parturition of ketosis cows and the association between the rumen microbiome and host energy metabolism. The study included 810 rumen content samples and 789 serum samples from day − 21 and 21 relative to calving day from 61 ketosis cows and 84 healthy cows.

Results In ketosis cows, the rumen bacterial composition after parturition changed dramatically and needed a longer time to restore. The molar proportions of propionate were lower in ketosis cows than those in healthy cows on days 3 and 7 and negatively correlated with the serum β-hydroxybutyrate (BHBA) levels. The fermentation sub-pathway of propionate metabolism and partial glucogenic amino acid pathways were downregulated on day 3. *Prevotella*, *UBA1066*, and microbiota diversity indices regulate serum BHBA and glucose (GLU) levels via arginine, alanine, glycine, or propionate. Propionate administration to ketosis cows potentially decreased the serum BHBA concentration.

Conclusions Collectively, we found rumen disruption happened after calving among ketosis cows, and insufficient glycogenic substrates, such as propionate, may be related to ketosis development. The study findings have implications for the relationship between rumen microbiome dynamics and host energy metabolism, which lays the foundation for the future rumen microbiome investigation for improving postpartum management in cows.

Keywords Dairy cow, Peripartum period, Energy metabolism, Ketosis, Rumen microbiome, Glucogenic precursors

†Fanlin Kong and Shuo Wang contributed equally to this work.

*Correspondence:
Shengli Li
lishengli@cau.edu.cn
Full list of author information is available at the end of the article

Background

Mammals transitioning from pregnancy to lactation experience marked physiological [1, 2] and metabolic [3] changes to support fetal and neonatal development and lactation launch. The overproduction of milk in dairy cows to levels exceeding the needs of calves is essential for meeting human food requirements [4]. However, 30–50% of postpartum dairy cows are unable to cope with the huge output and mobilization of energy and protein, resulting in metabolic disorders or postpartum diseases (such as ketosis, milk fever, displaced abomasum, retained placenta, uterine infections, and lameness) [5]. These diseases are a common concern in dairy farms, causing considerable economic and animal welfare losses [6]. The average lifespan of dairy cows is only 3 to 4 years [7], which is remarkably shorter than that of cows under natural conditions (20 years) [8].

Ketosis is a notorious metabolic disease in postpartum cows and is defined as the overexpression of ketone bodies and concurrent low blood glucose [9]. More than 20% of postpartum dairy cows exhibit ketosis [10]. An excessive circulation of ketone bodies is related to compromised reproductive and productivity performance [11] and potentially induces other postpartum diseases [12, 13]. Maternal effects in ketosis cows consequently depress growth parameters in the offspring [14]. The average cost per case of ketosis is US $289 [10]. The pathogenesis of ketosis has been investigated [9, 12]. After calving, energy output for milking and maintenance increases more rapidly than the increase in energy intake, creating a negative energy balance and mass body fat and protein mobilization. The hepatic oxidation of non-esterified fatty acids (NEFA), which are derived from adipose stores, can contribute to maintenance and milking requirements. However, the excess acetyl CoA from NEFA oxidation uses a limited amount of oxaloacetic acid in the tricarboxylic acid cycle and produces excess ketone bodies [9]. Hence, the body's levels of oxaloacetic acid and glucose dictate the products of acetyl CoA. For dairy cows, approximately 90% of glucose is generated by gluconeogenesis, 50–60% of which is derived from ruminal propionate [15, 16]. Propionate is produced from three microbial pathways (fermentation, amino acid catabolic, biosynthetic pathway) [17, 18]. Hence, its ruminal production depends primarily on the abundance and species of microbes. However, it is still unknown if dynamic changes in the rumen microbiome during the transition period (3 weeks before and after calving) affect the occurrence and progression of ketosis.

The rumen microbiome is predominated by fibrolytic microbes during the peripartum period and by amylolytic and proteolytic microbes during the postpartum period [19]. Similar to the host, the rumen microbiome also needs a transition period (approximately 14 days) to stabilize after parturition [20]. Interestingly, the shortening of this transition period using rumen microbiota transplantation technology in a previous study revealed that the rumen microbiome is associated with host energy metabolism [21]. A large data set including 277 dairy cows also indicated that the rumen microbial composition presents the variation in ketone bodies better than that by host genetics [22]. Indeed, two cross-sectional studies including ketosis cows on different days after calving revealed a decrease in the abundance of propionate-producing microbes [23, 24], whereas that of butyrate-producing microbes increased in ketosis cows, regardless of the time after calving [24]. However, longitudinal investigations indicate that the rumen microbiota composition is dramatically altered after calving [20, 25, 26]. Fecal microbiota analyses of ketosis cows revealed that the majority of the genes involved in branched amino acid metabolism in the gut microbiota are significantly altered on day 14 rather than those on day 7 [27]. A recent longitudinal study also stressed the importance of sample collection time [28]. Thus, the conclusions of a rumen microbiome study involving dairy cows in the peripartum period may be dependent on the sample collection time. Furthermore, the dynamic changes in carbohydrate and lipid metabolism indices of transition dairy cows are inconsistent and complex [11, 19, 29, 30]. For example, longitudinal data of blood NEFA and β-hydroxybutyrate (BHBA) levels suggest that the mean times of maximum NEFA and BHBA concentrations after calving are day 6.8 and day 9.6, respectively [29]. Thus, the elevated concentrations of one metabolite should not be extrapolated to suggest elevated concentrations of the other metabolite. A study investigating the association between rumination time and milk yield also reported that the relationship differs across weeks for postpartum dairy cows [30]. Hence, a large-scale, longitudinal cohort study in dairy cows is needed to determine the role of the rumen microbiome in carbohydrate and lipid metabolism during the postpartum period. Additionally, metagenomics can only reveal the "functional potential" of a microbiome [31]. Hence, using metabolomics and absolute quantification polymerase chain reaction (PCR) for metabolite and microbiota profiling in the rumen can more precisely identify the host-microbiome interactions.

We hypothesized that the special transition way of the rumen microbiome from parturition to the postpartum period contributes to ketosis development by regulating host metabolism. Here, we collected 810 rumen content samples and 789 serum samples from 61 ketosis cows and 84 healthy controls from −21 day to +21 day and integrated the bacterial composition profiles and serum

energy metabolism indices, along with the rumen fermentation parameters to establish the correlation. Based on 16S rRNA gene sequencing results, multi-omics tools (metagenomics sequencing and metabolomics) were used to further elucidate the potential mechanisms involved and the role of propionate in ketosis development. Our study aimed to elucidate the role of the ruminal microbiome in the energy metabolism of peripartum cows and understand the pathogenesis of ketosis during the perinatal period. Our results offer novel strategies for dairy cow management involving rumen microbiome intervention to improve metabolic adaptation.

Methods

Animal and experimental design

The experiment was conducted at a commercial dairy farm (39°93′N, 113°18′E, Datong, China), and all cows were raised in an intensive system. Initially, this farm had approximately 7000 Holstein dairy cows and could provide enough ketosis cows to collect samples in a short period and reduce environmental interferences. According to the farm protocol, cows are raised in a pen during the close-up period and would be transferred to the delivery pen after calving. The postpartum care was given in the delivery pen within 1–2 days, which included feeding an oral bolus (Bovikalc bolus, Boehringer Ingelheim, MO, USA) containing $CaCl_2$ and $CaSO_4$ (43 g of Ca), measuring rectal temperature (M900 Thermometer, GLA Agricultural Electronics, Inc., CA, USA), and drenching 300-mL liquid propylene glycol orally using a drench gun. After calving, the postpartum cows were transferred to a lactating pen within 2 days. The feed ingredients and nutrient compositions are presented in Table S1, and the formula was prepared according to the nutrient requirements of the dairy cattle [32]. After calving, all cows were fed thrice a day (0800, 1400, and 2000 h) and milked thrice a day (0700, 1300, and 1900 h).

The experiment was performed between October and December 2022, and the study design is presented in Fig. 1. According to the expected calving date, a total of 211 multiparous Holstein dairy cows were enrolled in our study. After exclusion, 145 dairy cows were used in the final analysis (Table S2). For consistency, a fixed veterinarian director was employed to diagnose all diseases except ketosis. The diseases are defined in Table S2. Blood samples were obtained via the coccygeal vessels using blood collection needles and EDTA evacuated tubes (10 mL, Beijing Hua Xia Heng Yuan Technology Co., Ltd., Beijing, China) when cows returned to their pen after morning milking. Immediately after collection, the BHBA concentrations were measured using a bovine-specific electronic BHBA handheld meter (Nova Vet, Nova Biomedical Corporation, MA, USA), which was validated for use in dairy cows with high accuracy and precision [33]. The BHBA concentrations were measured on days − 21, 1, 3, 7, 14, and 21. Cows with a BHBA level ≥ 1.2 mmol/L in at least one blood sample were diagnosed with ketosis. Finally, a total of 61 dairy cows were diagnosed with ketosis (KET), and 84 dairy cows were healthy without any other disease (CON). The cohort description is presented in Table S3. Based on the predicted calving day, the means and standard deviations (SDs) of the actual sampling day on day − 21 were day − 19.1 ± 3.91 (min ~ max, 10 ~ 31) and − 19.4 ± 4.65 (min ~ max, 11 ~ 31) for the CON and KET groups, respectively. Regardless of the exact hour of the calving day, samples of day 1 were collected on the day following parturition.

Production performance

Milk was collected three times a day using the DeLaval Rotary E500 milking system (Tetra Laval Group, Tumba, Sweden), and the daily total milk production was calculated except for day 1. The fixed and professional CowSignals Pro measured body condition scores (BCSs) on days − 21, 1, 3, 7, 14, and 21 using the method of Edmonson et al. [34]. BCS was recorded on a scale from 1 (thin) to 5 (fat) in increments of 0.25. From day − 21, we collected diet samples weekly and stored them at − 20 °C. We mixed the diets and analyzed their nutrient compositions, according to a previous study [35]. The results are shown in Table S1.

Serum collection and parameters measurement

On days − 21, 1, 3, 7, 14, and 21, blood samples were collected via the coccygeal vessels using blood collection needles and no-anticoagulant evacuated tubes (10 mL, Beijing Hua Xia Heng Yuan Technology Co., Ltd., Beijing, China) when cows returned to their pen after morning milking. Following this, the samples were centrifuged (4000 × g, 15 min, 4 °C) to obtain serum and stored at − 20 °C to further determine the biochemical indices after 2 months. The NEFA, glucose (GLU), and triglyceride (TG) levels were determined using a fully automatic biochemical analyzer (GF-D200, Gaomi Analytical Instrument Co. Ltd., Gaomi, China) combined with commercial kits (A042-2–1, Nanjing Jiancheng Bioengineering Institute, Nanjing, China). The serum concentrations of the 20 amino acids were determined according to a previous study [36].

Rumen content collection and measurement of fermentation parameters

The overview of samples is shown in Fig. S1. On days − 21, 1, 3, 7, 14, and 21, we collected the rumen

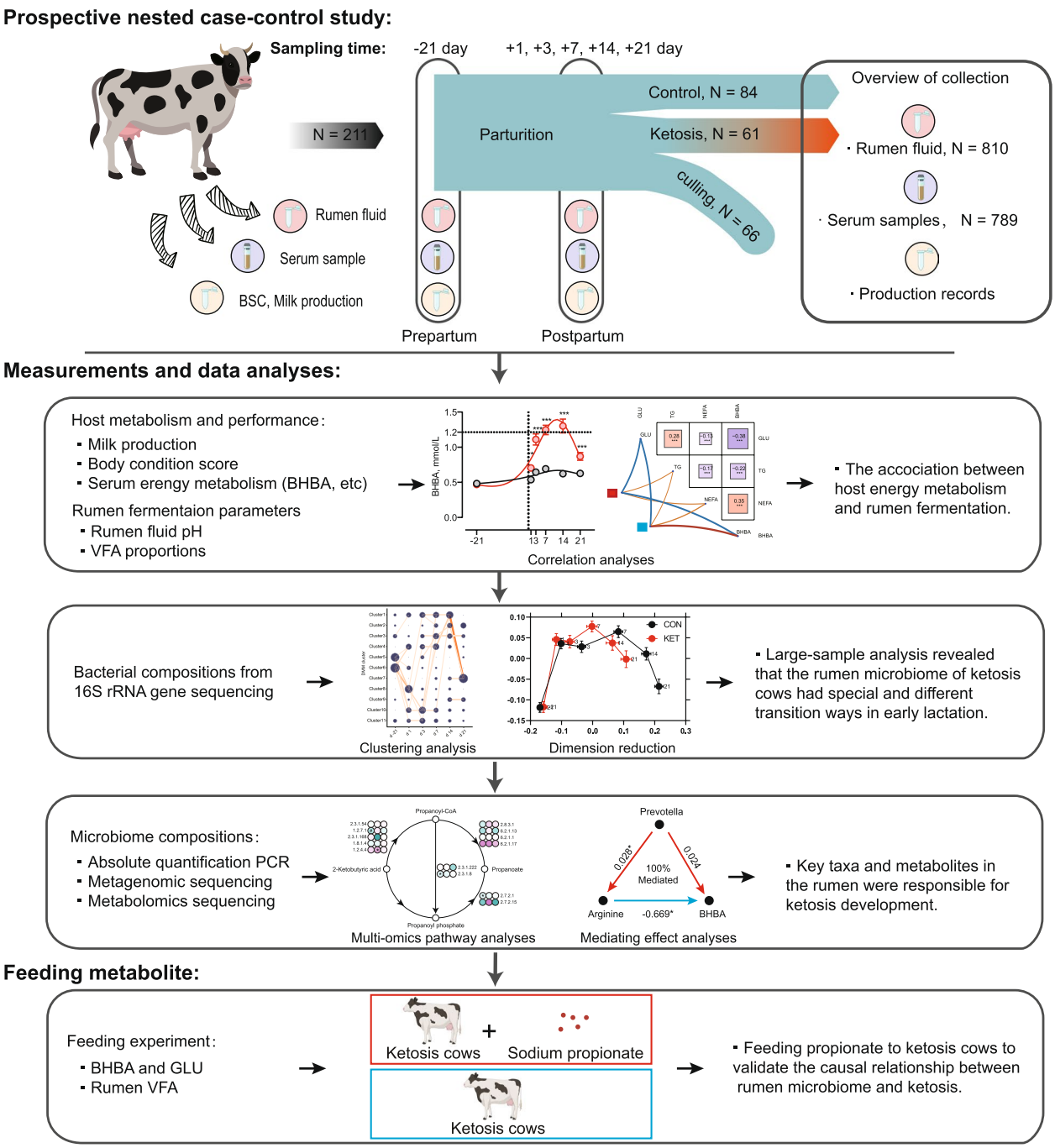

Fig. 1 Schematic representation of the study cohort design and the analysis process flow

content samples via oral intubation (Wuhan Anscitech Animal Husbandry Technology Co., Ltd., Wuhan, China) and 50-mL injector (Beijing Hua Xia Heng Yuan Technology Co., Ltd.) when cows returned to their pen after morning milking. A total of 810 rumen fluid samples were used in this study (Fig. S1). The initial 50-mL rumen content was discarded to avoid saliva contamination, and the subsequent 50 mL from individual cows was immediately used to measure the pH value using a Testo 206 pH meter (Testo, Inc., PA, USA). Further, 15-mL aliquot was stored in a storage tube at − 20°C to measure rumen fermentation parameters, and a 1.8-mL aliquot ($n = 3$) was stored in a storage tube at − 80°C for 16S rRNA, metabolome, and metagenome sequencing after 2 months. The

concentrations of volatile fatty acids (VFA) including acetate, propionate, butyrate, isobutyrate, valerate, and isovalerate were analyzed using the method of Wang et al. [37]. Briefly, the rumen fluid samples were thawed at 25 °C and centrifuged for 15 min at 16,000 × *g* at 4°C (centrifuge 5804R, Eppendorf Corporate, Oldenburg, Germany). We removed 1-mL supernatant into a 1.5-mL centrifuge tube and added 200-μL metaphosphoric acid (25%, v/v, Beijing Yili Fine Chemicals Co., Ltd., Beijing, China). After incubation on an ice bath for 30 min, the mixture was centrifuged for 10 min at 16,000 × *g* at 4°C (centrifuge 5804R, Eppendorf Corporate). Finally, we removed 1-mL supernatant into an injection bottle with a cap and analyzed the VFA concentrations and profiles using an Agilent G689N gas chromatograph and Agilent G7683 autosampler (Agilent Technologies, Inc., CA, USA). Individual standard VFA samples with 99% purity were used (Sigma A6283, Sigma P1386, Sigma I1754, Aldrich B103500, Aldrich 129542, Sigma V9759, Merck KGaA, Darmstadt, Germany).

DNA extraction, 16S rRNA gene sequencing, and data processing

DNA in the rumen content from days − 21, 1, 3, 7, 14, and 21 was extracted using a DNeasy PowerSoil Kit (cat. no. 47014, Qiagen, Hilden, Germany) and used for 16S rRNA gene and metagenome sequencing. The quantity and quality of the extracted DNA were evaluated using a NanoDrop NC2000 spectrophotometer (Thermo Fisher Scientific Inc., MA, USA), and the results are presented in Table S4. For 16S rRNA sequencing, the V3–V4 region of the bacterial 16S rRNA was PCR amplified using 20-ng DNA and Platinum Hot-Start PCR master mix (Thermo Fisher Scientific Inc.), 338F (5′-ACTCCTACGGGAGGCAGCA-3′), and 806R (5′-GGACTACHVGGGTWTCTAAT-3′). PCR amplicons were purified with Vazyme VAHTS™ DNA Clean Beads (Vazyme Biotech Co., Ltd., Nanjing, China). Finally, pair-end 2 × 250-bp sequencing was performed on the NovaSeq 6000 platform (Illumina, Inc., CA, USA).

For 16S rRNA sequencing, the raw data was processed using QIIME 2 (v 2023.5) [38]. First, raw sequence data were demultiplexed using the demux plugin followed by primer cutting with cutadapt plugin [39]. Further, we used DADA2 plugin to merge, denoise paired end reads, and remove chimera [40]. Non-singleton amplicon sequence variants were aligned with mafft [41]. Taxonomy was assigned to the amplicon sequence variant (ASV) using the Naïve-Bayes classifier in the feature-classifier plugin and against the SILVA database (v 138) [42]. Before diversity analysis, all samples were rarefied to 31,239 (95% read count of sample with minimum read count, Fig. S2). Raw data have been deposited in the NCBI database (PRJNA1116614, SRR29185432–SRR29186241).

Absolute quantification PCR

Thirteen cows per group were selected for absolute quantification (AQ) of the rumen microbiome using AQ-PCR. DNA in the rumen samples from days 3, 7, and 14 was extracted using the Mag-Bind Soil DNA Kit (200) (cat.: M5635-02, Omega Bio-tek, Inc., GA, USA). The concentration and purity of microbial DNA were measured using ND-2000 (Thermo Fisher Scientific Inc.), and the results are presented in Table S5. AQ-PCR was performed as described by Adebayo et al. [43]. The forward and reverse primers used were as follows: 5′-ACTCCT ACGGGAGGCAG-3′ (F) and 5′- GACTACCAGGGT ATCTAATC-3′ (R) for bacteria [44], 5′-GCTTTCGWT GGTAGTGTATT-3′ (F) and 5′-CTTGCCCTCYAATCG TWCT-3′ (R) for protozoa [45], 5′-CCGGAGATGGAA CCTGAGAC-3′ (F) and 5′-CGGTCTTGCCCAGCT CTTATTC-3′ (R) for methanogens [46], and 5′-GAG GAAGTAAAAGTCGTAACAAGGTTTC-3′ (F) and 5′-CAAATTCACAAAGGGTAGGATGATT-3′ (R) for fungi [47]. Samples were assayed in triplicate, and the standard curves met the following requirements: $R > 0.99$ and amplification efficiency > 80%. The final copy numbers of individual microbes per gram of dry matter of solid contents were determined.

Metagenomic sequencing and data processing

Rumen samples on days 3, 7, and 14 from the 13 cows used for AQ-PCR were randomly selected from each group for metagenomics analysis. The extracted total DNA was processed to construct metagenome shotgun sequencing libraries with insert sizes of ~ 400 bp using Illumina TruSeq Nano DNA LT Library Preparation Kit (Illumina, USA). Each library was sequenced using an Illumina NovaSeq™ X Plus platform (Illumina, USA) with PE150 strategy at Personal Biotechnology Co., Ltd. (Shanghai, China).

For metagenomics data processing, sequencing adapters were removed from raw reads using Cutadapt (v 1.2.1) [48]. Then, low-quality reads were trimmed using a sliding-window algorithm in fastp (v 0.23.2) [49]. Reads were aligned to the bovine genome using Minimap2 (v2.24-f1122) to remove host contamination [50]. Following this, taxonomical classifications of metagenomic sequencing reads from each sample were performed using Kaiju (v1.9.0) against a GTDB-derived database (v 207) [51]. Reads assigned to metazoans or viridiplantae were removed for downstream analysis. Megahit (v1.1.2) was used for the assembly of reads in each sample using the meta-large preset parameters [52]. The generated contigs were pooled together and clustered using Mmseqs2 (v15) with "easy-linclust" mode, setting the sequence identity threshold to 0.95 and covering residues of the shorter contig to 90% [53].

The lowest common ancestor taxonomy of the nonredundant contigs was obtained by aligning them against the NCBI-nt database using mmseqs2 with "taxonomy" mode, and contigs assigned to Viridiplantae or Metazoa were dropped in the following analysis. Prodigal (v2.6.3) was used to predict the genes in the contigs [54]. CDS sequences of all samples were clustered using the "easy cluster" mode of mmseqs2, setting the protein sequence identification threshold to 0.95 and covering residues of the shorter contig to 90%. Then, the reads were mapped onto the predicted gene sequences using Minimap2 and featureCounts to count the number of reads aligned to the gene sequences for each gene [55]. The unit of abundance was present and calculated as transcripts per kilobase per million mapped reads (TPM). The functionality of the nonredundant genes was obtained by annotation using mmseqs2 with the "search" mode against the Kyoto Encyclopedia of Genes and Genomes (KEGG) and CAZy protein databases. KO was obtained using KOBAS [56]. Raw data have been deposited in the NCBI database (PRJNA1116614, SRR29188398–SRR29188472, SRR29188744, SRR29188745).

Metabolomics sequencing and data processing

Samples used for metagenomics sequencing were also selected for metabolomics analysis. A total of 100-μL rumen content was taken and mixed with 400-μL extraction solution (MeOH: CAN, 1:1 (v/v)). Then, the mixed solution was vortexed for 30 s, sonicated for 10 min in a 4°C water bath, and incubated for 1 h at − 40°C, for protein separation. The samples were then centrifuged at 13,800 × g for 15 min at 4°C, and the supernatant was transferred into a glass vial for further analysis. The quality control samples were used to evaluate system stability and data reliability. The samples were analyzed in both positive and negative modes of electrospray tandem mass spectrometry. Analyses were performed using Vanquish UHPLC (Thermo Fisher Scientific Inc., MA, USA) coupled with an Orbitrap Exploris 120 mass spectrometry (Thermo Fisher Scientific Inc., MA, USA). Raw MS data were converted to MzXML files using ProteoWizard MS Convert, and the XCMS R package using R (version 4.3.1) was used to detect feature retention time correction and alignment. The MS/MS data identified were matched with the BiotreeDB database (v3.0).

Sodium propionate supplementation experiment

This experiment was conducted in another commercial dairy farm (37°29′N, 114°54′E, Xingtai, China), which housed approximately 8000 Holstein dairy cows and could provide sufficient ketosis cows to collect samples in a short period. Precisely, the peripartum cows which were disease-free during the last parity were enrolled in this experiment. On day 7 after calving, blood samples were obtained via the coccygeal vessels using blood collection needles and no-anticoagulant evacuated tubes (10 mL, Beijing Hua Xia Heng Yuan Technology Co., Ltd., Beijing, China) when cows returned to their pen after morning milking. The BHBA concentrations were measured as mentioned above until 10 ketosis cows were analyzed. We assigned these cows into two groups according to parity and milk production in the last parity. The ketosis + sodium propionate (SP) group (mean ± SD: parity, 3.4 ± 0.89; milk production, 11,159 ± 1068.6 kg) was administered 240 g/day sodium propionate (Shandong Guante Biological Engineering Co., Ltd., Heze, China). Sodium propionate (120 g) was dissolved in 350-mL water and fed to the cows. The applications were administered orally twice a day during morning and evening feeding from day 7 to day 14 after calving. The ketosis group (mean ± SD: parity, 3.0 ± 0.71; milk production, 11,346 ± 1338.6 kg) served as the placebo (700-mL water per day).

During days 7 to 14, blood samples were collected via the coccygeal vessels using blood collection needles and no-anticoagulant evacuated tubes (10 mL, Beijing Hua Xia Heng Yuan Technology Co., Ltd., Beijing, China) when cows returned to their pen after morning milking and before administering SP. The GLU concentration was measured via a bovine-specific electronic GLU handheld meter (CentriVet GK, ACON Biotechnology Co., Ltd, Hangzhou, China), and BHBA concentrations were measured as mentioned above. On days 7, 8, 10, 12, and 14, rumen samples were collected when cows returned to their pen after morning milking, and before administering SP, and were used to analyze VFA concentrations as described above.

Statistical and bioinformatic analyses

The background information was compared between two groups using a two-sided Mann–Whitney *U*-test. The production performance data (milk production and BCS), serum energy indices, rumen fermentation parameters (pH and VFA), and AQ-PCR data on day − 21 were analyzed using *t*-test, and these data on days 1, 3, 7, 14, and 21 were analyzed together using the PROC MIXED procedure of SAS version 9.4 (SAS Institute Inc., Cary, NC, USA). Fixed effects included treatment, time, and the interaction of treatment and time. The cow was included as a random effect. The results were visualized using GraphPad Prism 9.3 (GraphPad, MA, USA). The VFAs were presented as the molar proportion (%) and concentrations (mmol/L). Mantel

and correlation analysis between serum parameters and rumen fermentation parameters were conducted and visualized on the Genes Cloud platform (https://www.genescloud.cn). *P*-value < 0.05 was considered significant.

For 16S rRNA sequencing data, alpha-diversity indices including Shannon and Chao1 at the ASV level were calculated using QIIME2 (v 2023.5) [38] and visualized using GraphPad prism 9.3 (GraphPad, MA, USA). Beta-diversity analysis was performed among different groups and time points to reveal the dissimilarity of bacterial communities using PERMANOVA analysis based on the Bray–Curtis method and visualized via principal coordinate analysis (PCoA). Furthermore, PC1 and PC2 were centroids with standard error of the mean (SEM) to expose the external differences. Next, PERMANOVA analysis based on the Bray–Curtis method was used to calculate the dissimilarity between subsequent time points in each group. Dirichlet multinomial mixtures (DMM) was used to determine the key phases of bacterial progression [57], which bins samples based on bacterial community structure using R code (version 4.3.1) modified from Stewart et al. [58]. The appropriate number of clusters was determined based on the lowest Laplace approximation score. A heatmap was used to show the relative abundances of the bacterial composition of different clusters in R (version 4.3.1). The top 20 genera that contributed the most to the accuracy of the DMM are shown in the order of importance in Cleveland's dot plot. The number of samples occupying a DMM cluster at each point was plotted to visualize temporal changes in community types during the peripartum period. The inter-cluster transition rate was quantified and visualized using a Markov chain based on an R script [59] (version 4.3.1).

For metagenomics sequencing data, the proportion of bacteria, eukaryotes, archaea, and viruses, and α-diversity based on the read level of each sample were calculated, to maximize the utilization of sequencing data and then compared using the Wilcoxon test with $P < 0.05$ being considered as significant. Following this, we used Procrust analysis to show the significance of group separation using PCoA. Then, Linear discriminant analysis Effect Size (LEfSe) analysis was used to filter the significantly altered KEGG pathways at different time points. The threshold was linear discriminant analysis (LDA) score > 2. Spearman correlation was conducted among different genera. *P*-value < 0.05 was considered statistically significant. The fold change used in this study was calculated as KET/CON. The propionate metabolism pathway was divided into three sub-pathways according to previous studies [17, 18].

For metabolomics data, orthogonal projections to latent structures discriminant analysis were used to calculate variable importance for the projection (VIP) value. Wilcoxon test was applied to calculate statistical significance. The metabolites with $VIP > 1$ and $P < 0.05$ were considered differential metabolites at each time point. The functions of these metabolites were then matched against the KEGG database. Different abundance score plot was used to explore the up or downregulated pathways.

The mediating effect model (MEM) was used to construct the regulation (model rumen microbial taxa-metabolites-host energy metabolism) by process plugins in SPSS (v29, Hangzhou, China) [60]. The Shannon and Chao1 indices and taxa which predominantly contributed to propanoate metabolism and amino acid metabolism (contribution rate > 1%) were enrolled in this model as dependent variables. Metabolites including propionate and significantly different glucogenic amino acids were considered as mediators. BHBA and GLU were considered as dependent variables.

Results

Rumen microbial fermentation was associated with energy metabolism

We prospectively included 211 dairy cows before calving, 61 of which eventually developed ketosis, as diagnosed based on the serum BHBA levels after calving (Fig. 1). The 84 healthy cows served as the control group. Initially, we determined the serum BHBA, GLU, NEFA, and TG concentrations, to characterize the dynamic changes in energy metabolism during the peripartum period (Fig. 2a). The postpartum data analyzed using the MIXED procedure is presented in Table S6. The postpartum average BHBA concentration was significantly higher, and the postpartum average GLU concentration was significantly lower in the KET group than those in the CON group (Fig. 2a, Table S6). The average maximum value of BHBA was observed on day 14 in the KET group. Conversely, the average minimum value of GLU was observed on day 14 (Fig. 2a). There was no difference in milk production between the groups (Fig. S3a). The average NEFA concentration in the KET group was higher than that in the CON group during the postpartum period (Fig. 2a, Table S6). Moreover, an interaction between time and treatment was observed for BCS, and it was lower in the KET group than that in the CON group on day 21 (Fig. S3b).

Except for butyrate and "other VFA" proportions, all rumen fermentation parameters were significantly affected by treatment (Fig. 2b, c, d, e). The average rumen pH during postpartum was higher in the KET than that in the CON group (Table S6). The total VFA (TVFA),

acetate, propionate, butyrate, and other VFA concentrations were significantly higher in the CON group than those in the KET group (Table S6). An interaction between time and treatment was detected for the acetate-propionate (A-P) ratio (Fig. 2d). Particularly on days 3 and 7, the A-P ratio was higher in the KET group than that in the CON group. The propionate concentration and proportion were affected by the interaction between time and treatment (Fig. 2c and e). The average propionate proportion during the postpartum period in the KET group was lower than that in the CON group (Table S6). The propionate concentrations on days 1 and 3 (Fig. 2c), and propionate proportions on days 3 and 7 (Fig. 2e), were significantly lower in the KET group than those in the CON group. Further, we performed Mantel analysis between VFA proportion, concentration, and serum indices (Fig. 2f). The findings revealed that the VFA proportion and concentration correlated with BHBA and GLU concentrations (Fig. 2f). Among individual VFAs, the propionate concentration negatively correlated with the BHBA concentration and had the maximum *r*-value among all the other VFAs (Fig. 2g).

Special transition way of rumen bacteria in ketosis cows

We further sequenced the bacterial composition and diversity for all the rumen samples. Following quality control processes and bioinformatic processing, a total of 810 rumen samples from 145 dairy cows were included to investigate temporal changes in rumen bacterial profiles. The median read count was 65,020 (*IDR*: 57,004–73,054, Fig. S2). Firstly, compared to the CON group, the KET group showed a higher Shannon index on days 7, 14, and 21 and a higher Chao1 index on days 7 and 21 (Fig. 3a). Moreover, beta-diversity comparison using PCoA via Bray–Curtis distance and PERMANOVA methods revealed that the KET group differed significantly from the CON group on days 1, 3, 7, 14, and 21, and the difference increased with time (Fig. 3b). Finally, dissimilarity analysis between two time points showed that the dissimilarities from day − 21 to day 1 and day 1 to day 3 were higher in the KET group than those in the CON group and subsequently decreased from day 3 to day 7 and day 7 to day 14 (Fig. 3c).

To identify changes in the bacterial composition during the peripartum period, we performed unsupervised clustering of taxonomic data into different types using DMM. The 11 DMM clusters were determined according to the lowest Laplace approximation (Fig. S4a). The top 30 most abundant genera in each sample were clustered by community types (Fig. 3d), and the top 20 most important genera for clustering rumen bacterial communities are presented in Fig. 3e. *Prevotella* was the predominant genus involved in clustering (Fig. 3e), and clusters 5 and 6 were dominant before calving in both the KET and CON groups (Fig. 3f, g). After calving, majority of the CON group cows were present in cluster 8 on day 1 and quickly transitioned to clusters 1, 3, and 4 on day 3 and reached clusters 1, 2, and 3 on day 7 (Fig. 3f). Finally, most of the cows transitioned to clusters 2, 7, and 9 on days 14 and 21 (Fig. 3f). Compared with the CON group, most of the cows in the KET group were present in clusters 10 and 11 on days 1 and 3 (Fig. 3g). Subsequently, these cows transitioned to cluster 1 on day 14, which was later than that for the CON group (day 7) (Fig. 3g). On day 21, the KET group mainly included clusters 2, 7, and 9, similar to the CON group (Fig. 3g). To quantify the shift of different clusters during the peripartum period, we used a Markov chain-based approach to model the enterotype transition probabilities (Fig. S4b, c). In the KET group, cluster 10 was connected to clusters 5, 6, and 8 and clusters 1 and 4 (Fig. S4c).

Dynamic changes in rumen microbiota composition

The 16S rRNA sequencing for the big data set revealed that dairy cows with ketosis exhibited a special dynamic change in rumen bacteria. Hence, we further performed AQ-PCR and metagenomics to determine alterations in

(See figure on next page.)

Fig. 2 Changes and associations of rumen microbial fermentation and energy metabolism in healthy (CON) and ketosis (KET) cows during the peripartum period. **a** Longitudinal change in serum energy metabolism indices, including β-hydroxybutyrate (BHBA), glucose (GLU), non-esterified fatty acid (NEFA), and triglyceride (TG) in ketosis and healthy cows during the peripartum period. Lowness was used to create a smooth line. Data are presented as mean ± standard error of mean (SEM). Statistical significance was calculated for day-21 data using unpaired two-tailed *t*-tests. A mixed model was used to analyze the postpartum data. **P* < 0.05; ***P* < 0.01; ****P* < 0.001. **b**, **d** Longitudinal change in pH and ratio of acetate to propionate concentration in ketosis and healthy cows during the peripartum period. Lowness was used to create a smooth line. Data are presented as mean ± SEM. Statistical significance was calculated using unpaired two-tailed *t*-tests. **P* < 0.05; ***P* < 0.01; ****P* < 0.001. **c**, **e** Longitudinal changes in concentration and proportion of volatile fatty acid (VFA) in the ketosis and healthy cows during the peripartum period. Boxplots represent the 10th and 90th percentiles. Data are presented as mean ± SEM. Statistical significance was calculated for day-21 data using unpaired two-tailed *t*-tests. A mixed model was used to analyze the postpartum data. **P* < 0.05; ***P* < 0.01; ****P* < 0.001. **f** Mantel test analysis between serum indices and VFA proportion and concentration in the ($n = 745$). Color gradients indicate Pearson's correlation coefficients. Edge width corresponds to the Mantel's *r*-value, and edge color denotes the statistical significance. **P* < 0.05; ***P* < 0.01; ****P* < 0.001. **g** Pearson correlation between individual VFA proportions and serum BHBA concentration in the KET group ($n = 308$). The shaded areas surrounding the lines indicate the 90% confidence intervals

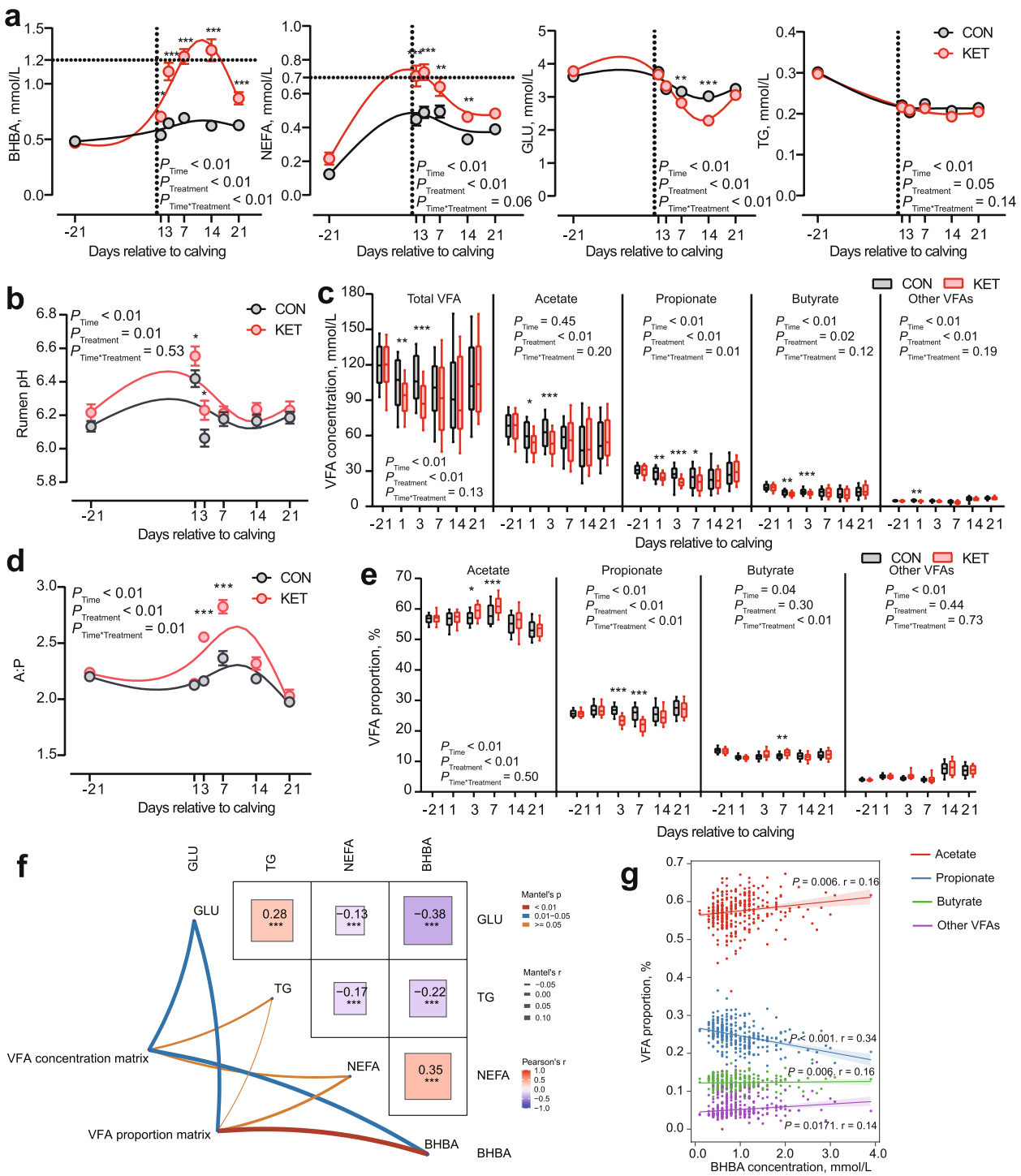

Fig. 2 (See legend on previous page.)

the functions and composition of microbes. Only the copy number of bacteria was significantly affected by treatment and interaction (Fig. 4a). The average copy number of bacteria during the postpartum period was lower in the KET group than that in the CON group (Table S6), particularly on days 7 and 21 (Fig. 4a). Further, the proportion of microbes calculated using metagenomics based on read count showed that the proportion of individual microbes was not significantly different (Fig. 4b). The Chao1 index of bacteria was higher in the KET group than that in the

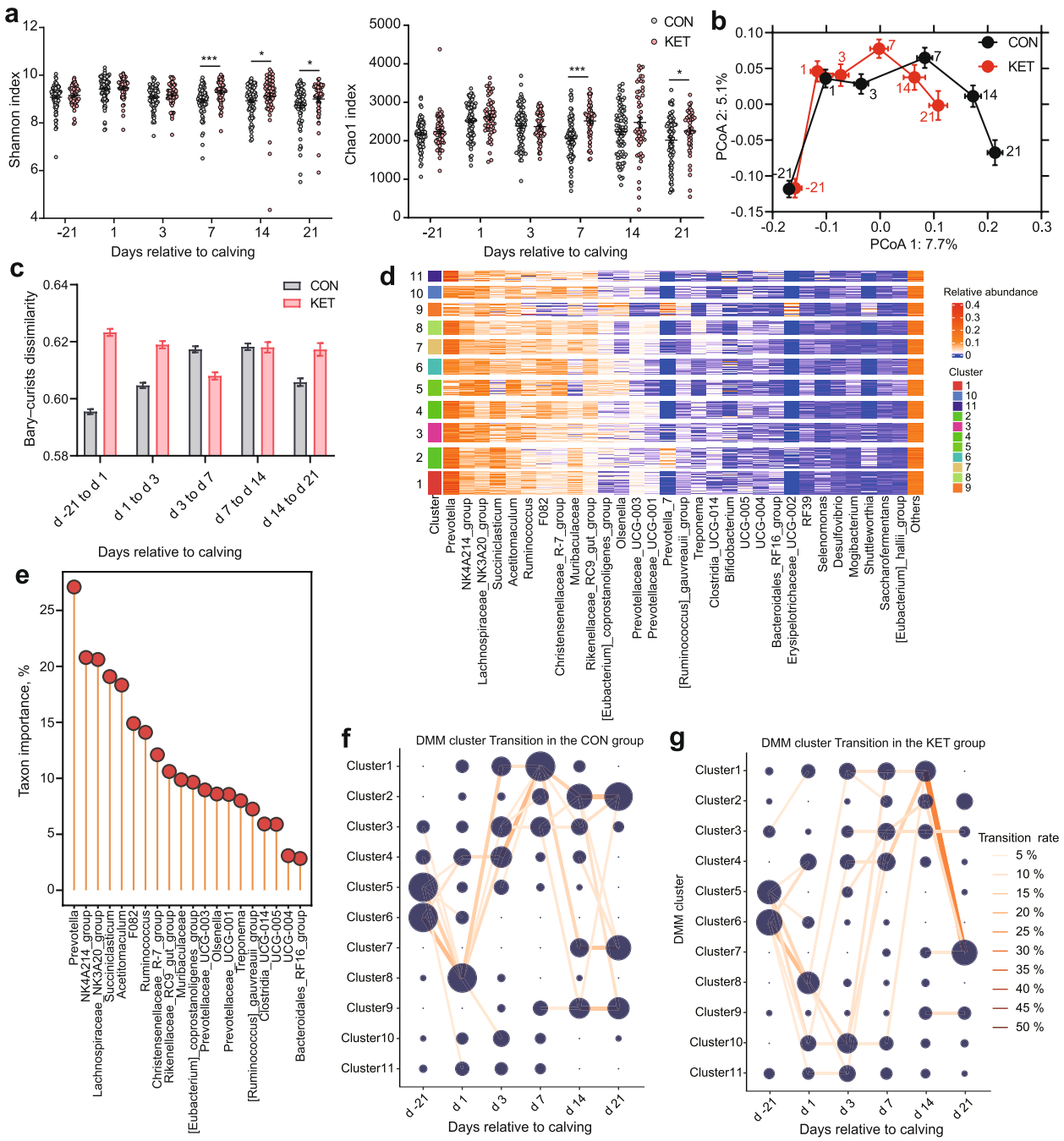

Fig. 3 Overview of the transition way of rumen bacteria diversity and composition in ketosis (KET) and healthy (CON) cows during the perinatal period. **a** Dynamic change in Shannon and Chao1 indices. The alpha-diversity indices were calculated based on the amplicon sequence variant (ASV) level. Data are presented as mean ± SEM, and every point represents one sample. Statistical significance was calculated using the two-tailed Wilcoxon rank test. *$P < 0.05$; **$P < 0.01$; ***$P < 0.001$. **b** The principal coordinate analysis (PCoA) of Bray–Curtis dissimilarities obtained on the ASV level. The red data labels indicate the KET group, and the black data labels indicate the CON group. The circles and error bars indicate the mean and SEM of the mean. *P*-values for the comparison of rumen bacterial composition on the day − 21, 1, 3, 7, 14, and 21 are 0.139, 0.004, 0.005, 0.001, 0.001, and 0.001 (PERMANOVA test with 999 permutations). **c** Microbiota stability over time. Bray–Curtis dissimilarities were calculated within each group between each pair of subsequent timepoints. Data are presented as mean ± SEM. **d** Heatmap shows the top 30 relative abundances of genera for each sample. Samples are grouped using Dirichlet multinomial mixtures (DMM) cluster to visualize the genera enriched or reduced on an average in each DMM cluster. **e** Cleveland plot shows the 20 genera in order of importance which contributed to the accuracy of the DMM. **f**, **g** Dot flow diagram showing the temporal progression of microbiota cluster membership. Transitions between clusters are plotted. The transition rate is determined by dividing the number of transitions towards a given cluster by the total number of transitions within each time window. Edges and nodes are scaled by the number of included samples

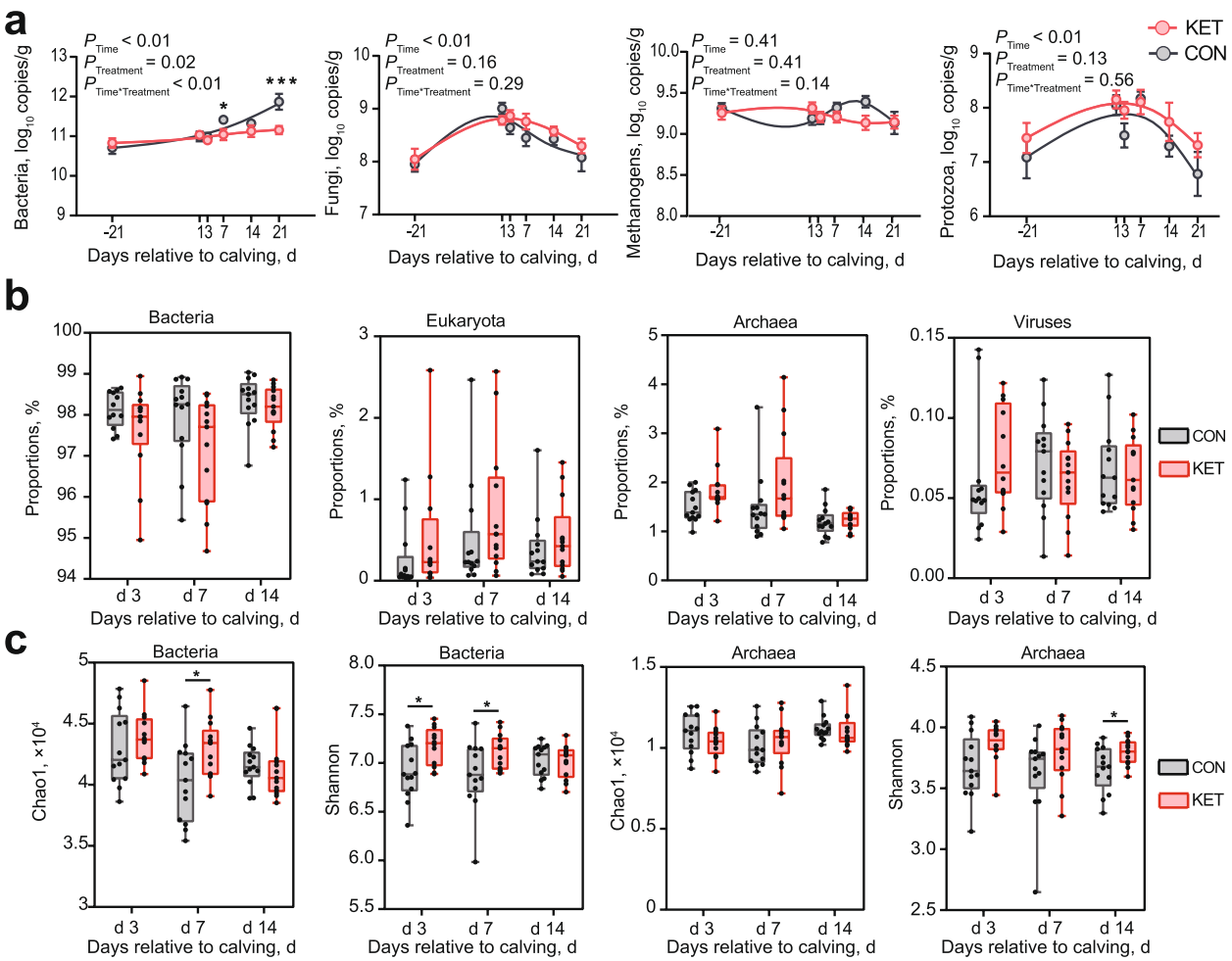

Fig. 4 Dynamic changes in the rumen microbial profile in ketosis (KET) and healthy (CON) cows during the perinatal period. **a** Absolute quantification of rumen microbiota using PCR from prepartum to postpartum. Lowness was used to create a smooth line. Data are presented as mean ± SEM. Statistical significance was calculated for day-21 data using unpaired two-tailed *t*-tests. A mixed model was used to analyze the postpartum data. **P* < 0.05; ***P* < 0.01; ****P* < 0.001. **b** Relative quantification of rumen microbiota based on the read count using metagenomics on days 3, 7, and 14. The boxplots show the mean (centerline), quartiles (box limits), and max to min range (whiskers). Dots correspond to individual samples. *P*-values were calculated using the two-tailed Wilcoxon rank-sum test. **P* < 0.05; ***P* < 0.01; ****P* < 0.001. **c** Alpha diversity of bacteria and archaea on days 3, 7, and 14. The Shannon and Chao1 indices were calculated based on the read counts. The boxplots show the mean (centerline), quartiles (box limits), and max to min range (whiskers). Dots correspond to individual samples. *P*-values were calculated using the two-tailed Wilcoxon rank-sum test. **P* < 0.05; ***P* < 0.01; ****P* < 0.001

CON group on day 7 (Fig. 4c). Compared to the Shannon indices of eukaryote and viruses (Fig. S5), the Shannon index of bacteria was higher in the KET group than that in the CON group on days 3 and 7. The Shannon index in Archaea was higher in the KET group than that in the CON group on day 14 (Fig. 4c).

Microbial functions of amino acid and carbohydrate metabolism decreased in ketosis dairy cows

Gene level expression based on TPM revealed that the microbiota was significantly different between the two groups on days 3, 7, and 14, while the microbiota function was altered only on day 3 (Fig. 5a). M2 from Procrustes analysis also indicated inconsistencies in the composition and function on days 3, 7, and 14 (Fig. 5a, M2 > 0.6). Thus, we further filtered the functions enriched in different groups, and the results revealed that the number of significantly different functions of rumen microbiota decreased from day 3 to 14 (Fig. 5b). However, no common significantly different pathway was found among the three time points (Fig. 5c). The different pathways mainly included metabolism at KEGG level 1 (Fig. 5d).

Fold change revealed that pathways at KEGG level 3, including long-term potentiation, glutamatergic synapse,

various types of N-glycan biosynthesis, glycosaminoglycan degradation, DNA replication, base excision repair, mismatch repair, and homologous recombination, were enriched in the KET group. These pathways mainly included glycan biosynthesis and metabolism, replication, and repair at KEGG level 2 (Fig. 5e). Further, pathways from the LefSe analysis enriched in the CON group were visualized using a heatmap (Fig. 5f). These belonged to metabolism pathways, wherein metabolism of starch and sucrose, glyoxylate and dicarboxylate, and propanoate belong to carbohydrate metabolism, and arginine biosynthesis, lysine biosynthesis, tyrosine metabolism, phenylalanine metabolism, phenylalanine, tyrosine and tryptophan biosynthesis belong to Amino acid metabolism (Fig. 5f).

Glucogenic amino acids and their metabolic pathways were downregulated in the rumen of ketosis cows

The metabolite profiles of the rumen microbiome were determined using metabolomics. After filtering the significantly different metabolites, the significantly altered pathways were identified (Fig. 6a). Interestingly, protein digestion and absorption and several amino acid metabolism pathways including lysine degradation, alanine, aspartate, and glutamate metabolism, and beta-alanine metabolism were upregulated on day 3 in the CON group. The pathways common among the three-time points were autophagy — animal, autophagy — other, glycosylphosphatidylinositol-anchor biosynthesis, Kaposi sarcoma-associated herpesvirus infection, purine metabolism, pyrimidine metabolism, and retrograde endocannabinoid signaling (Fig. 6b). We further filtered pathways which were significant based on both metagenomics and metabolomics at individual time points. Among these, glycerophospholipid metabolism, pantothenate and CoA biosynthesis, and starch and sucrose metabolism were significant on day 3 and antifolate resistance on day 7 (Fig. 6c). Considering the consumption of a high-starch diet (22.61% starch) during the postpartum period (Table S1), carbohydrate metabolism was affected in the KET group.

We summarized the fold change (KET/CON) of metabolic pathways in all amino acids using rumen metagenomics, the abundance of ruminal amino acids using metabolomics, and the serum amino acid concentrations (Fig. 6d). In the KET group, the rumen microbial pathways including arginine biosynthesis, phenylalanine, tyrosine, tryptophan biosynthesis, and tyrosine metabolism pathways were significantly downregulated on day 3. The ruminal concentrations of glucogenic amino acids including arginine, alanine, glycine, and tyrosine were significantly decreased on day 3 in the KET group compared to those in the CON group (Fig. 6d). Meanwhile, the serum concentrations of histidine and glucogenic amino acids, including arginine and alanine, decreased on days 3, 7, and 14 in the KET group than those in the CON group. The serum total amino acid (TAA) concentration decreased on days 3 and 7 in the KET group than that in the CON group.

The fermentation pathway to produce propanoate was downregulated in the rumen of ketosis dairy cows

Among the significantly different pathways, the relative carbohydrate metabolism pathways were downregulated in the KET group (Fig. 7a). After dietary intake, cellulose, hemicellulose, pectin, and starch in feedstuffs were degraded by ruminal microbes (Fig. 7a). Further, propanoate can be produced via three microbial pathways. Comparisons of the relative abundance of CAZyme genes are shown in Fig. S6, and the relative abundance of carbohydrate esterases (CE) was lower on day 3 in the KET group than that in the CON group.

We calculated the percentage of genes involving individual propanoate sub-pathways using metagenomics. Among all rumen fluid samples, the average abundance of amino acids catabolic, fermentation, and biosynthetic pathways accounted for 57.25, 33.78, and 8.97% of the total abundance, respectively (Fig. 7b).

Moreover, the fold change (KET/CON) in the enzymes of genes identified using metagenomics, and metabolites identified using metabolomics, was determined (Fig. 7c). The abundance of three enzymes involved in isoleucine

(See figure on next page.)

Fig. 5 Dynamic changes in microbial functions of the rumen in ketosis (KET) and healthy (CON) cows during the postpartum period. **a** Procrustes analysis and PERANOVA based on PCoA and Bray–Curtis to test the consistency between function and composition of the rumen microbiota on days 3, 7, and 14. The microbial function (hollow circle) and composition (solid circle) for each sample were connected by a line. $P < 0.05$ for Procrustes was considered as consistency between composition and function. $P < 0.05$ for PERANOVA was considered a significant separation between the two groups at each time point. **b** Linear discriminant analysis effect size analysis identifying significantly different pathways between the two groups on days 3, 7, and 14. The cutoff value was linear discriminant analysis (LDA) > 2 and $P < 0.05$. **c** Venn plot to find the common significantly different pathways on days 3, 7, and 14. **d** The profiles of significantly different pathways on Kyoto Encyclopedia of Genes and Genomes (KEGG) level 1 from different time points. **e** The fold change of pathways enriching in the KET group using LefSe analysis. The data was calculated by $\log_2$(KET/CON). **f** Heatmap plot of normalized relative abundance of metabolism pathways enriched in the CON group using LefSe analysis. Data are presented based on Z-score normalization

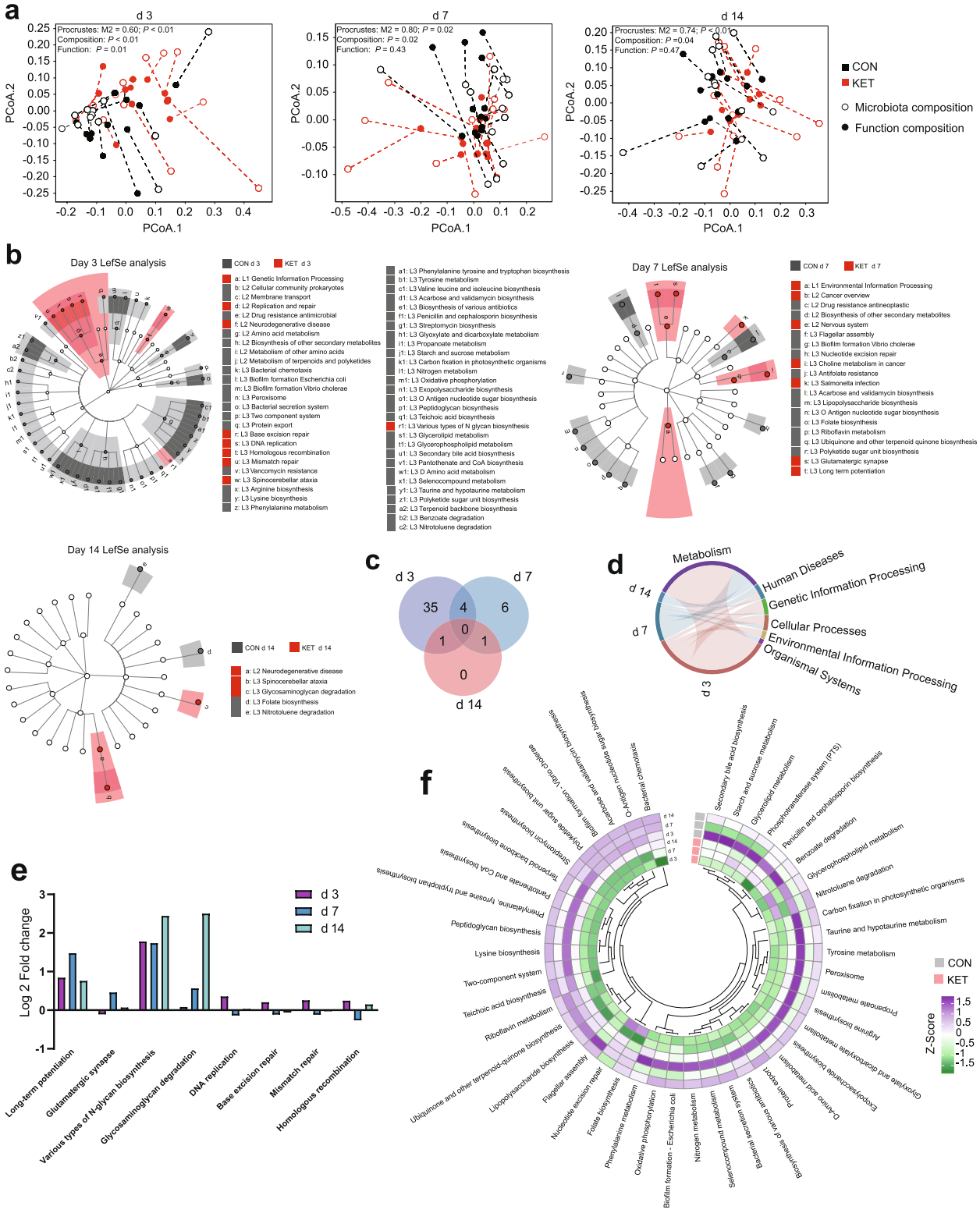

Fig. 5 (See legend on previous page.)

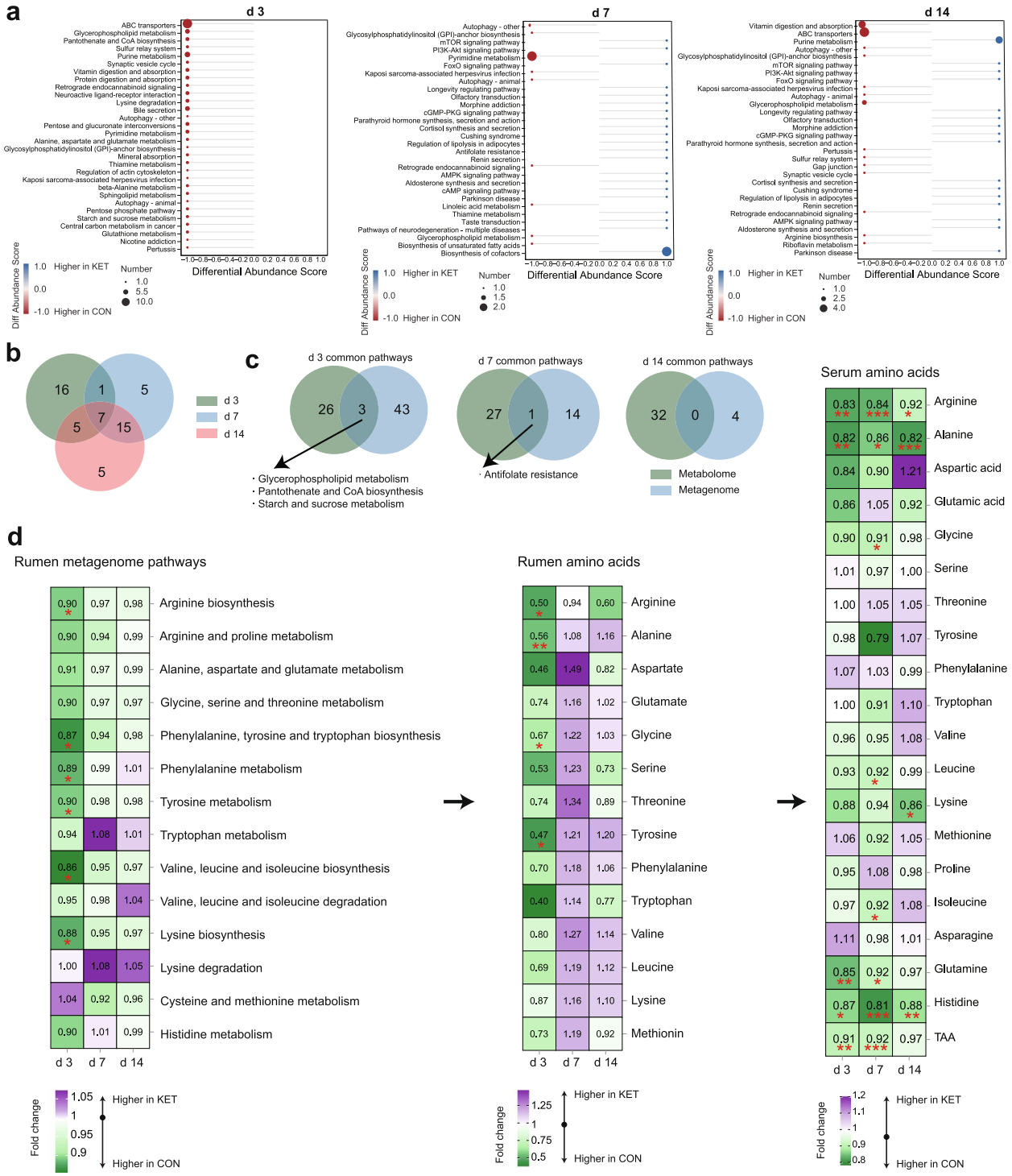

Fig. 6 Glucogenic amino acids and their metabolic pathways were downregulated in the rumen of ketosis cows. **a** The top 30 significantly different pathways on days 3, 7, and 14 after calving were determined using metabolomics. The pathways are sorted based on the number of differential metabolites. The differential abundance scores of – 1 and 1 indicate downregulated (red) and upregulated (blue) pathways, respectively, in the KET group compared with those in the CON group. **b** The common pathway among different days determined using metabolomics. **c** The common pathway between metagenomics and metabolomics analyses on an individual day. **d** The fold change (KET/CON) for the abundance of amino acids from metabolomics and microbial gene abundance of their pathways from metagenomics on days 3, 7, and 14. *P*-values were calculated using the two-tailed Wilcoxon rank-sum test. **P* < 0.05; ***P* < 0.01; ****P* < 0.001

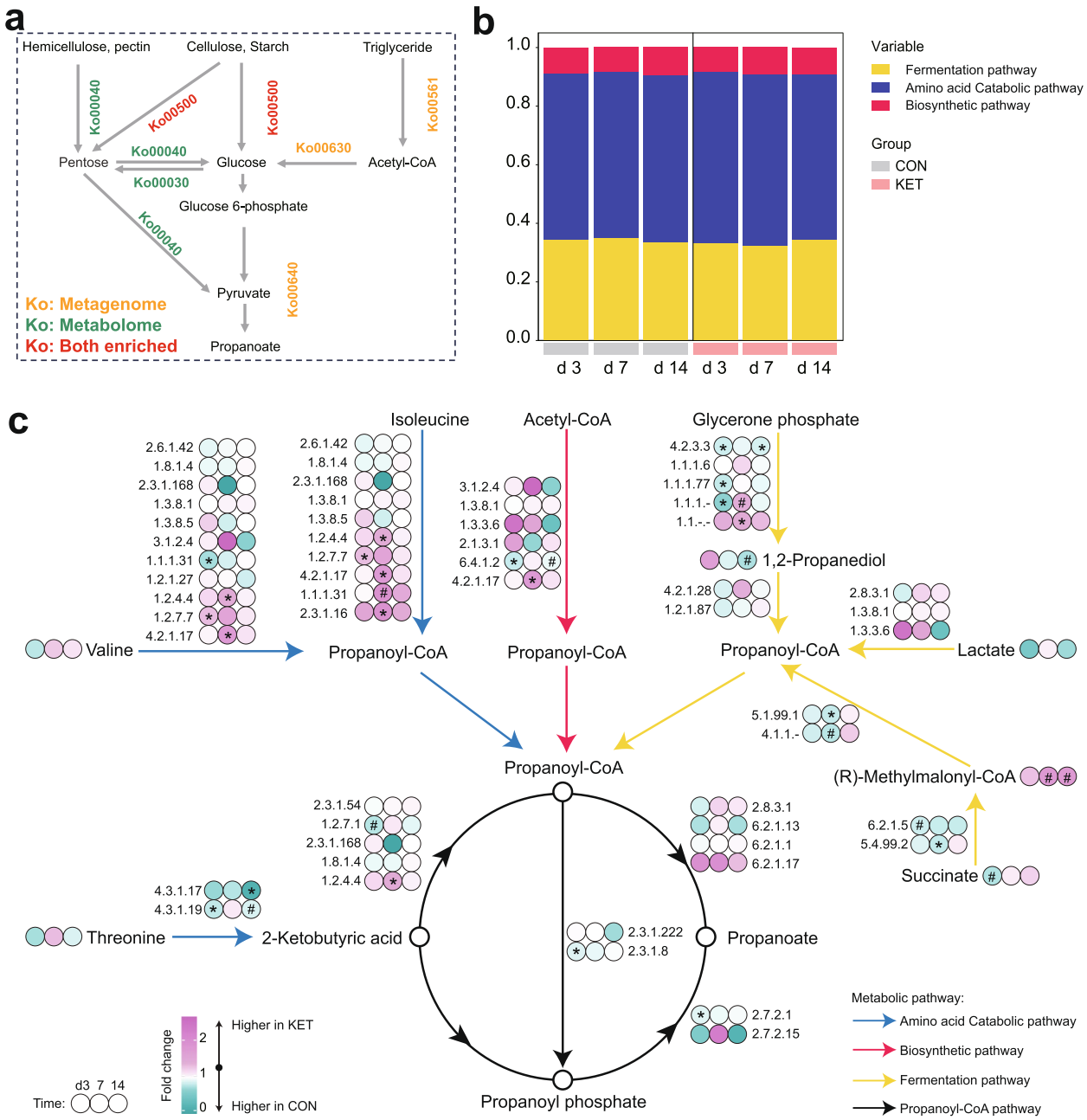

Fig. 7 Propanoate metabolism in carbohydrate metabolism was downregulated in the rumen of ketosis cows. **a** Schematic summary for the downregulated carbohydrate metabolism pathways in the rumen of the KET group using metagenomics and metabolomics. The downregulated pathways from metagenomics were filtered by the total relative abundance of genes in the pathways. The downregulated pathways from metabolomics were obtained by matching the significantly downregulated metabolites against the KEGG database. **b** The proportions of different propanoate metabolism pathways on days 3, 7, and 14. The microbial genes involved in propanoate metabolism were selected and divided into three different producing pathways. **c** Dynamic change in the metabolites and enzymes involved in the propanoate metabolism pathways. The circle color indicates the fold change between the KET and CON groups at each time point. The line color indicates the different sub-pathways of propanoate. *P*-values were calculated using the two-tailed Wilcoxon rank-sum test. #0.05 < *P* < 0.10; **P* < 0.05

catabolism and two enzymes in valine catabolism were significantly higher in the KET group than those in the CON group on day 7. In threonine catabolism, the levels of *EC*: 4.3.1.17 on day 14 and *EC*: 4.3.1.19 on day 3 were higher in the CON group than those in the KET group. Only one enzyme (*EC*: 6.4.1.2) in the biosynthetic pathway was downregulated in the KET group on day 3. For the fermentation pathway, the levels of three enzymes were significantly reduced, and that of one enzyme tended to be lower on day 3 in the KET group than those in the CON group. Moreover, the levels of two enzymes on day 7 and one enzyme on day 14 were reduced in the KET group. Finally, the products from three pathways were included in the propionyl-CoA pathway, and the abundance of *EC*: 2.7.2.1 and *EC*: 2.3.1.8 on day 3 were significantly lower in the KET group than those in the CON group.

The mediating effect model revealed that the rumen microbiota resulted in ketosis by decreasing the supply of glucogenic amino acids and propionate

Propionate and glucogenic amino acids are the precursors of GLU. Hence, we used MEM to elucidate the relation among the microbes, their metabolites, and GLU or BHBA, to clarify the pathogenesis. Firstly, we filtered the genera that predominantly contributed to amino acid and propanoate metabolism (contribution level > 1%) (Table S7). After difference analysis, the abundance of seven genera, including *Prevotella*, *Ruminococcus E*, *UBA1066*, *Sodaliphilus*, *CAG-103*, *Succiniclasticum*, and *Porcincola*, significantly reduced on one of the days 3, 7, and 14 and contributed to both amino acid and propanoate metabolism. In particular, the change matrix indicated that the abundances of all these genera were significantly decreased in the KET group on day 3 (Fig. 8a). The relative abundances of *Prevotella* on day 7 and *CAG103* on day 14 also decreased (Fig. 8a). Then, correlation analysis also revealed many positive correlations among these genera (Fig. 8b).

Finally, MEM showed that independent variables, including *Prevotella*, *UBA1066*, Chao1, and Shannon indices, correlated with mediating variables including propionate, arginine, glycine, and alanine, which eventually correlated with BHBA and GLU concentrations (Fig. 8c). The independent variables also had direct effects on BHBA and GLU concentrations (Fig. 8c). Arginine, propionate, and alanine were negatively associated with the BHBA concentration, and propionate was positively associated with the GLU concentration (Fig. 8c). According to the MEM conditions, 10 mediating effects were established, among which 6 were completely mediating effects (*Prevotella* → arginine → BHBA, *UBA1066* → propionate → BHBA, Shannon → Propionate → BHBA, *UBA1066* → Propionate → GLU, Chao1 → Propionate → GLU, and Shannon → Propionate → GLU), 2 were partially mediating effects (Chao1 → glycine → BHBA and Chao1 → propionate → BHBA), and 2 were masking effects (Chao1 → arginine → BHBA and Chao1 → alanine → BHBA) (Fig. 8d). Collectively, arginine potentially mediated the associations between *Prevotella* and BHBA and Chao1 and BHBA (Fig. 8d). Propionate potentially mediated the associations between *uba1066* and BHBA, Chao1 and BHBA, Shannon and BHBA, *UBA1066* and GLU, Chao1 and GLU, and Shannon and GLU (Fig. 8d). Alanine and glycine potentially mediated the association between Chao1 and BHBA (Fig. 8d).

Feeding sodium propionate to ketosis cows to validate the role of rumen microbiota and its metabolites in the development of ketosis

Ketosis cows were filtered on day 7 after calving and fed SP from day 7 to day 14 (Fig. 9a). The dynamic change in blood BHBA, GLU, and rumen VFAs concentrations are presented in Fig. 9, and the results of statistical analysis are presented in Table S8. After feeding SP, the average BHBA concentration was lower, and the average GLU concentration was higher in the ketosis + SP group than those in the CON group (Table S8). The BHBA and GLU concentrations were affected by the interaction between time and SP treatment (Fig. 9b and c). We found that the BHBA concentration decreased from day 7 to day 14 in the ketosis + SP group (Fig. 9b). The BHBA concentration was lower in the ketosis + SP group than that in the

(See figure on next page.)

Fig. 8 Mediating effect model revealed the serum BHBA and GLU concentrations regulated by the genera and diversity of rumen microbiota by decreasing the supply of glucogenic substrates. **a** Fold change matrix for the fold change (KET/CON) of genera which contributed to the amino acid and propanoate metabolism pathways predominantly on days 3, 7, and 14 and downregulated in the KET group on one of the days 3, 7, and 14. *P*-values were calculated using the two-tailed Wilcoxon rank-sum test. *$P < 0.05$; **$P < 0.01$; ***$P < 0.001$. **b** Correlation matrix of rumen genera which contributed more than 1% to the amino acid pathway and propanoate metabolism pathway and were downregulated in the KET group on one of the days 3, 7, and 14. Spearman's correlation was used, and $P < 0.05$ was considered statistically significant. *$P < 0.05$; **$P < 0.01$; ***$P < 0.001$. **c** Sankey diagram of a correlation between two variables in the mediating effect model. Only significant associations ($P < 0.05$) are retained. In this model, the independent variables can affect dependent variables directly or through mediating variables. **d** Chart showing the established mediating effect models. The figures above the arrowed lines indicate the regression coefficient. The asterisk indicates the significant regression relation. *$P < 0.05$; **$P < 0.01$; ***$P < 0.001$. The numbers in the triangle indicate the mediation effects

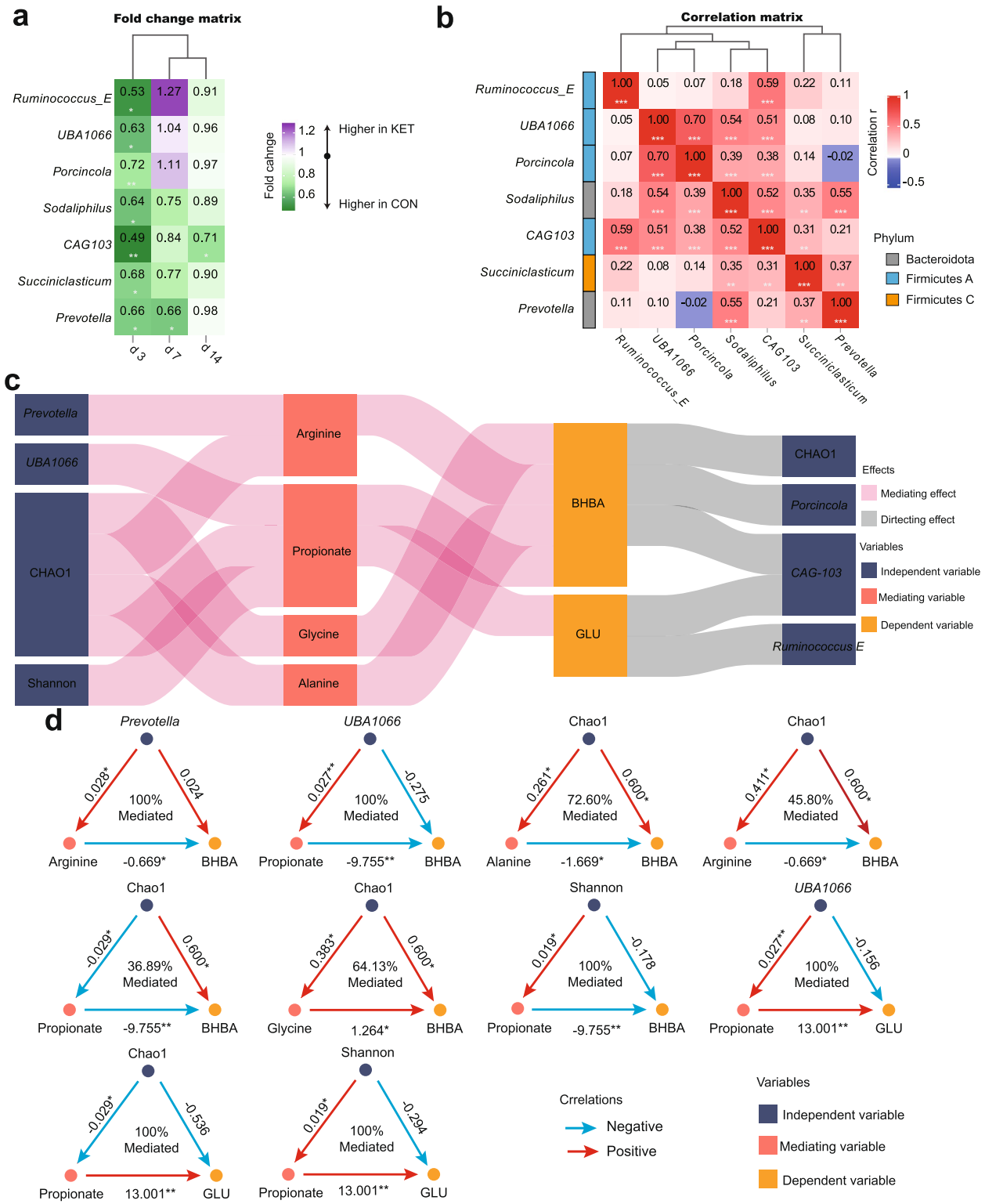

Fig. 8 (See legend on previous page.)

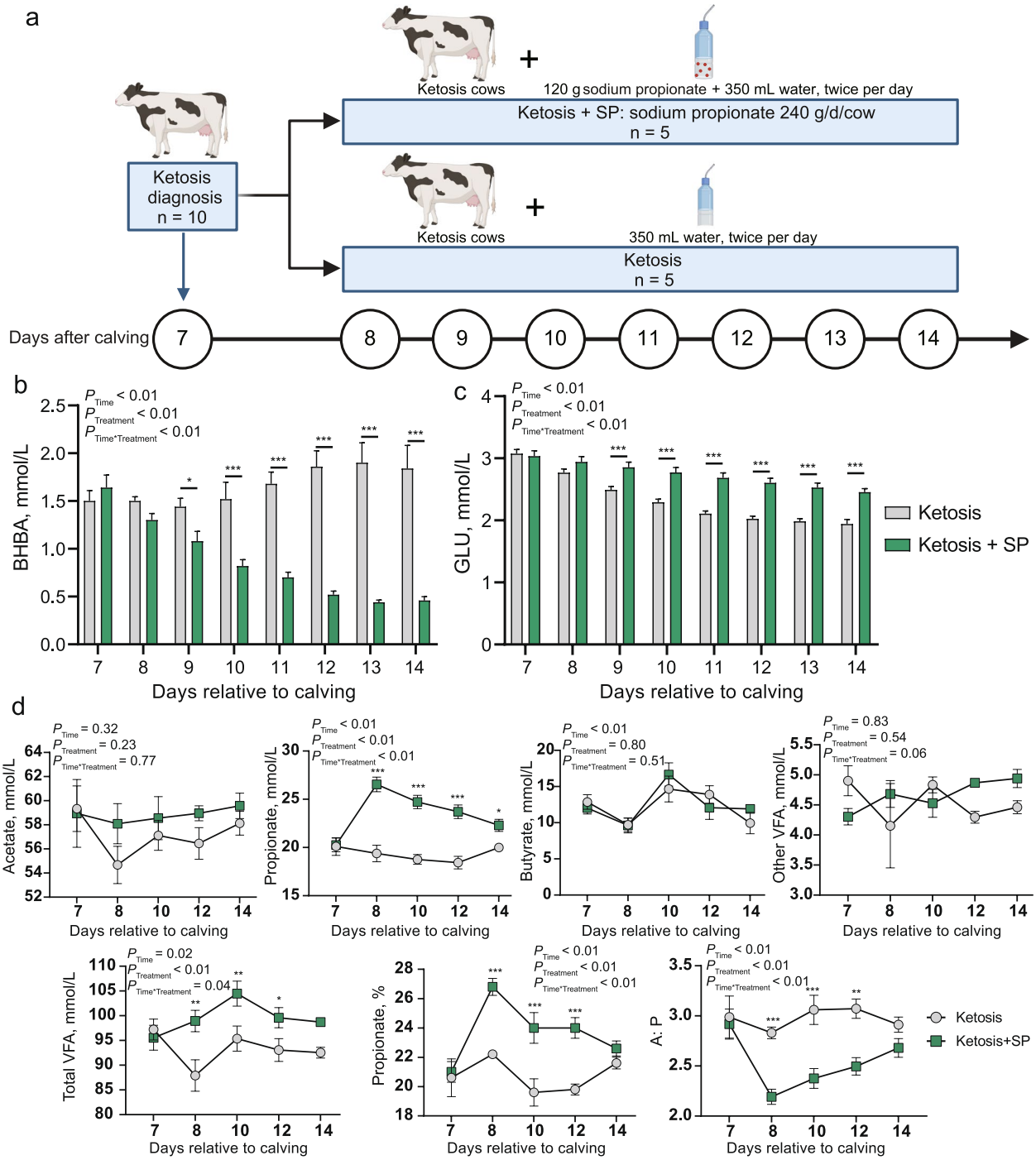

Fig. 9 Effect of sodium propionate supplementation on blood BHBA and GLU concentrations and rumen fermentation parameters of ketosis dairy cows. **a** Schematic representation of the experiment. Ketosis + SP group indicates the ketosis dairy cows in this group administered 240 g/day sodium propionate. Ketosis group indicates untreated ketosis cows. **b**, **c** Effects of sodium propionate supplementation on blood BHBA (**b**) and GLU (**c**) concentration. Data are presented as mean ± SEM. Statistical significance was calculated for day-21 data using unpaired two-tailed *t*-tests. A mixed model was used to analyze the postpartum data. **P* < 0.05; ***P* < 0.01; ****P* < 0.001. **d** Effects of sodium propionate supplementation on rumen fermentation parameters. Data are presented as mean ± SEM. Statistical significance was calculated for day-21 data using unpaired two-tailed *t*-tests. A mixed model was used to analyze the postpartum data. **P* < 0.05; ***P* < 0.01; ****P* < 0.001

ketosis group from day 9 to day 14 (Fig. 9b). The GLU concentration was higher in the ketosis + SP group than that in the ketosis group from day 9 to day 14 (Fig. 9c).

We found an interaction between time and SP for propionate concentration and proportion, total VFA concentration, and A-P ratio (Fig. 9d). The propionate concentrations were higher in the ketosis + SP group than those in the ketosis group on days 8, 10, 12, and 14. In the ketosis + SP group, the propionate concentration decreased gradually from days 8 to 14. TVFA concentration and propionate proportion were higher, whereas the A-P ratio was lower in the ketosis + SP group than those in the ketosis group on days 8, 10, and 12. The TVFA concentration and propionate proportion on day 14 were not significantly different between the two groups.

Discussion

Ketosis is one of the most prevalent diseases in dairy cows and induces other diseases during the peripartum period (3 weeks before and after calving) [11–13]. However, the endogenous causes of carbohydrate and lipid metabolism disorders remain unknown. It is considered that approximately half of the glucose is converted from glucogenic substances. To our knowledge, this is the first dynamic study to identify the association between rumen fermentation and host energy metabolism. Here, the deficiency of glucogenic substances from the rumen could be the key to increased ketone bodies in dairy cows. In ketosis cows, rapid and extensive mobilization of body fat, and the peaks in serum concentrations of BHBA and GLU, appeared later than those of NEFA, similar to a previous study [61]. The observational study indicated similar energy balances in ketosis and healthy cows. However, the milk fat content was higher in ketosis cows, which implies that the energy output in ketosis cows is higher than that in healthy cows [62]. Altered NEFA levels and BCS in our study indicated that more body tissue may be mobilized in ketosis cows to synthesize milk fat. Although milk production was consistent during the first 21 days in our study, a previous study found that ketosis cows exhibit a greater milking potential during the 305-day milking cycle [63]. The prevention of ketosis contributes to cow welfare as well as high milk production. Furthermore, our results highlight the importance of longitudinal investigations [11, 19, 29], as the various tracks of different serum indices.

After calving, the change in BHBA and GLU levels showed a similar trend. GLU deficiency diverts acetyl CoA from the tricarboxylic acid cycle to ketogenesis [9]. For dairy cows, propionate from rumen microbial synthesis is the most important and dominant glucogenic substance; other compounds, including glucogenic amino acids and glycerol, are mainly sourced from microbial synthesis and diet [15]. Wang et al. [23] identified that ketosis cows have lower acetate, propionate, and butyrate concentrations in the rumen than the lowest VFA concentration in healthy cows during the peripartum period. Eom et al. [64] also found low acetate and propionate levels in ketosis cows. These studies, along with our correlation analysis between VFA proportion and serum indices, revealed that significantly altered rumen fermentation in ketosis cows, which was associated with GLU and BHBA production. Furthermore, we expressed the quantity of VFA by molar proportion, and only propionate levels were low in ketosis cows on days 3 and 7. Propionate also showed the maximum correlation coefficient with BHBA concentration. Therefore, our results suggest that ruminal production of VFA, particularly propionate, was associated with BHBA production.

Host-microbial interactions in dairy cows regulate host metabolism [21] and induce diseases [65]. VFA is a rumen microbial product. Hence, we further analyzed the dynamic change in bacterial composition and diversity in the big data set, to identify differences between ketosis cows and healthy cows. In healthy cows, the microbial diversity decreases after calving [20, 25, 26]. This may be attributed to a decrease in the retention time of rumen content and colonization of microbes due to a high-concentrate diet in the postpartum period [66]. Furthermore, this high-energy diet with a specific fermentation substance is associated with overgrowth and occupation of a range of bacterial taxa, thereby reducing the relative abundance of other taxa below detectable limits [20, 25, 26]. In ketosis cows, 16S rRNA and metagenomics sequencing revealed higher Chao1 and Shannon indices in our study, indicating that rumen microbiota became more complex and competitive but less specific to ferment the feed to support the host energy requirements [67]. This assumption was proved by the low absolute number of bacteria low TVFA and high pH values in our study, consistent with the findings of cross-sectional studies [24, 68]. Furthermore, dissimilarity analysis between two time points revealed the transition way of rumen bacteria in healthy cows was more moderate during the peripartum period and stable from day 14 to day 21, while it was more dramatic for ketosis cows at the beginning of lactation. Hence, we speculated marked ruminal microbiota disruption in ketosis cows after calving and further investigated alterations in the function of rumen microbiota using metagenomics and metabolomics, to elucidate the underlying mechanism.

Rumen microbiota is known to stabilize approximately 14 days after calving [19, 25], which was consistently observed in our study among healthy cows.

Interestingly, the dominant clusters on days 3, 7, and 14 were considerably different between the two groups. To investigate this phenomenon, we further analyzed the microbial functions and metabolites on these days. Although the rumen microbiota composition varied on days 3, 7, and 14, the function of the rumen microbiota was significantly different only on day 3. The inconsistency may be attributed to species from the same genus, identified as generalists [69]. Furthermore, multi-omics comprehensively elucidates the flow of information at different levels [70]. The replication and repair pathways are related to microbiota disruption under extreme environments, such as copper exposure [71] or humans with disease [72]. Majority of the pathways enriched in ketosis cows on day 3 belonged to replication and repair, in agreement with the findings of 16S rRNA sequencing that rumen microbiota disruption occurs after calving. Considering that the time of microbiota disruption was earlier than the time of the peak BHBA concentration, we speculated that the special route of rumen microbiota in ketosis cows may be associated with disease development, and further studies are needed to validate the causal relationship.

Cross-sectional studies have suggested altered gut microbiome composition in dairy cows with ketosis [22–24, 64, 68]. Microbial genes involved in butyrate production from pyruvate or acetyl-CoA and propionate production from succinate and lactate lead to ketosis by increasing BHBA precursors and, meanwhile, decreasing GLU supply [24]. Metabolomics further revealed that starch and sucrose metabolism and propanoate metabolism pathways were downregulated in ketosis cows [64]. Correspondingly, CE and a series of carbohydrate metabolism pathways from feed stuff to propanoate were downregulated on day 3 in the rumen of our study. Division of the propionate production pathway in microbiota into three parts revealed that the fermentation and threonine-derived pathway were downregulated, instead of the biosynthetic pathway and valine and isoleucine-derived pathway.

Seven genera with similar trends were involved in propionate deficiency, among which *Ruminococcus* and *Prevotella* negatively correlated with serum BHBA concentrations [24, 68] and were highly reliable biomarkers for predicting BHBA concentrations in milk [22]. *Prevotella* is a versatile microbe capable of processing various proteins and polysaccharides in the gut, and propionate is one of its fermentation products [73]. *Prevotella* also improves GLU metabolism by promoting increased glycogen storage in humans [74]. Interestingly, *Succiniclasticum* is relatively less abundant in ketosis cows, with no correlation with BHBA [68]. The transition of GLU and BHBA after calving may explain the relation between *Succiniclasticum* and BHBA. A review has concluded the function and product of *Ruminococcus_E* strains and indicated their ability to disintegrate and utilize various plant polysaccharides and produce acetate as a major metabolic product [75]. Hence, we speculated that the genus *Ruminococcus_E* may be involved in amino acid metabolism rather than propionate.

The genera *Sodaliphilus* and *Porcincola*, which are presented in the pig microbiota [76], have been poorly characterized within the rumen microbiome. More information is needed in the future to explain the role of these genera in rumen microbiota. Genus *UBA1066* named *Chordicoccus* included *Chordicoccus furentiruminis*, which has been isolated from the rumen content of steer fed a high-grain diet and produces succinic acid as a major fermentation product [77], suggesting it may be related to carbohydrate fermentation and propionate production. In summary, the different microbiota composition involved in carbohydrate fermentation in the rumen contributes to the differences observed in propionate metabolism and highlights the importance of several genera in improving glucose production and preventing postpartum ketosis in cows. Considering the disruption of rumen microbiota and several altered microbes in our study, it would be difficult to validate the role of these taxa in ketosis development. Hence, we conducted a feeding experiment for ketosis cows by feeding propionate, which is specifically a microbiota product. Our results revealed that propionate was an effective additive to alleviate the degree of ketosis and may prevent ketosis in cows. An early study explored the potential of SP as an additive and its ability to increase the rumen propionate concentration and decrease the serum GLU concentration [78]; however, the production level and diet composition of dairy cows have recently changed significantly. Furthermore, Oba et al. [79] suggested a dose–response effect of ruminal propionate infusion on dry matter intake by providing sodium propionate from 540 to 2699 g/day for postpartum dairy cows, since propionate is the fuel that potentially stimulates satiety and reduces feed intake in dairy cows [80]. Hence, the appropriate dietary dose of SP should be investigated in the future.

Metagenomics and metabolomics analyses revealed that amino acid metabolism and metabolism of other amino acid pathways at KEGG L 3 were enriched in healthy cows. The protein digestion and absorption pathway were also enriched in healthy cows. Rumen microbiota plays a key role in addressing the nitrogen requirement by supplying microbial proteins to dairy

cows, representing approximately half of the protein reaching the duodenum [81] and supplying nitrogen for synthesizing milk protein or transferring to energy, such as glucogenic amino acids [82]. A nitrogen balance experiment conducted by Daniel et al. [61] indicated that dairy cows lose approximately 60 g of nitrogen per day from calving to week 2. The decreasing milk protein content in cows with ketosis also indicates a deficiency of proteins or amino acids [62].

Amino acids perform diverse functions in the body. Glucogenic amino acids include nonessential amino acids, such as aspartic acid, asparagine, serine, glutamine, glutamic acid, alanine, tyrosine, and cysteine, and two essential amino acids, histidine and arginine [83]. The pathways and metabolites of glucogenic amino acids, such as arginine, alanine, glycine, and tyrosine, were markedly downregulated in ketosis cows. Using metagenomics and grouping cows using blood BHBA concentration on day 21, Wang et al. [24] reported no differences in any KEGG pathways at levels 1 or 2 in the rumen, which was similar to our results, with few pathways altered on day 21. Eom et al. [64] compared the rumen metabolome in three dairy cows and reported downregulated cysteine and methionine metabolism pathways in ketosis cows. Collectively, limited information is available regarding the rumen metabolome changes due to the small sample size and sampling time. Hence, we measured serum amino acid concentrations to prove the effect of the rumen microbiome on host metabolism relying on the positive linear relationship between amino acid supply and serum amino acid concentrations [84].

Fetter et al. [85] reported that the essential amino acid concentrations decreased after calving, and the nonessential amino acid concentrations increased in dairy cows, owing to the known role of nonessential amino acid as glucogenic precursors. In our study, the high serum TAA concentration in ketosis cows demonstrated that the mobilization of amino acids from the muscle was more severe in ketosis cows than that in healthy cows. Further, similar to our study findings, Wang et al. [86] found significantly decreased alanine, glutamine, and lysine concentrations in the plasma of ketosis cows. The same amino acids, including arginine and alanine, were significantly altered, both, in the rumen content and serum, indicating regulation of the rumen microbiome in host metabolism. Finally, significant alterations in amino acid concentrations were no longer limited to day 3 but were observed throughout the postpartum period. Liver biopsies revealed that the liver glycogen concentration decreased by 74% from day − 10 to day 10 [87]. Postpartum cows might have to mobilize skeletal muscle continuously to supply GLU, following the rapid exhaustion of glucogenic precursors. However, these changes in the liver have not been verified using gene expression. Further elucidation of the underlying mechanisms for regulating hepatic energy metabolism by rumen microbiota is needed. Using the MEM, we constructed a model including genera, their metabolites, and host energy metabolism indices to connect the rumen microbiome and host metabolism. *Prevotella*, *UBA1066*, and richness and diversity indices showed mediating effects to regulate BHBA and GLU via arginine, alanine, glycine, or propionate. A human study reported that gut disruption is associated with altered arginine metabolism and *Prevotella* might contribute to the change in arginine flux [88]. This phenomenon has also been observed in humans with Parkinson's disease with gut disruption [89]. Thus, rumen microbiota disruption in dairy cows after calving could impact subsequent glucogenic amino acid production. An intrinsic limitation of our study is that inferences on cause-consequence relationships remain challenging owing to the lack of a validation model. Further studies are needed to validate our findings. In addition, it has been reported that gut microbiome alterations led to postpartum immunosuppression in transition dairy [80]. It is essential to further explore the association between the rumen and intestinal microbiome and their cross-talk in postpartum dairy cows.

Conclusions

To our knowledge, this is the first study to perform a longitudinal assessment of the rumen microbiome in dairy cows with carbohydrate and lipid metabolism disorder during the peripartum period, particularly using the multi-omic method and big-data set which also includes rumen microbiota, metabolome, and host metabolism indices. Some cows initially exhibited rumen microbiota disruption after calving and needed a longer time to adapt, which altered the microbiota genes involved in propionate and glucogenic amino acid metabolism, subsequently decreasing the supply of glucogenic precursors. Our subsequent feeding experiment revealed that propionate is an effective glucogenic precursor to supply GLU and alleviate the severity of ketosis. Our study highlights the important role of the rumen microbiome in regulating host energy metabolism and in the pathogenesis of ketosis and suggests potential strategies for preventing ketosis by regulating the rumen microbiota or supplying special glucogenic precursors (such as propionate, arginine, and alanine).

Supplementary Information

The online version contains supplementary material available at https://doi.org/10.1186/s40168-025-02072-3.

Additional file 1: Table S1. The feed ingredients and nutrient composition of diets. Table S2. Summary of reasons for exclusion. Table S3. Cohort description. Table S4. Average yield and quality of DNA from rumen content samples used for 16S RNA and Metagenomics. Table S5. Average yield and quality of DNA from rumen content samples used for AQ-PCR. Table S6. Cohort study data were analyzed using the MIXED procedure. Table S7. The genera contributed more than 1% to amino acid and propanoate metabolism on days 3, 7, or 14. Table S8. Data from the sodium propionate supplementation experiment was analyzed using the MIXED procedure.

Additional file 2: Figure S1. Overview of the number of rumen fluid and serum samples from healthy (CON) and ketosis (KET) cows during the peripartum period. Figure S2. The process of sequence denoising and read count statistics for 16S rRNA V3-V4 sequencing. Figure S3. Milk production and body condition score changes in the healthy (CON) and ketosis (KET) cows during the peripartum period. Figure S4. Laplace value for different clusters and inter-cluster transition rate visualization using a Markov chain in Dirichlet multinomial mixtures (DMM) analysis. Figure S5. Changes in alpha diversity of eukaryota and viruses in rumen microbiota in ketosis (KET) and healthy (CON) cows on days 3, 7, and 14. Figure S6. Comparisons of the relative abundances of CAZyme genes in the rumen microbiota of healthy (CON) and ketosis (KET) cows on days 3, 7, and 14 relative to those on the calving day.

Acknowledgements
We thank Dr Yangyi Hao from China Agricultural University for suggestions of the structure of this manuscript.

Authors' contributions
F.L.K., S.W., Y.J.W., Z.J.C., H.J.Y., W.W. and S.L.L. designed the study. F.L.K., S.W., C.L., Y.L.B., D.W.D., and C.G. conducted all the experiments. F.L.K, S.W., and Y.J.Z. analyzed the data. F.L.K. and SW. wrote the manuscript. All authors revised and approved the final version of the manuscript.

Funding
This work was supported by the National Natural Science Foundation of China (32130100).

Data availability
The 16S rRNA gene sequencing raw data have been deposited in the NCBI database (PRJNA1116614, SRR29185432–SRR29186241). The metagenomics raw data have been deposited in the NCBI database (PRJNA1116614, SRR29188398–SRR29188472, SRR29188744, SRR29188745).

Declarations

Ethics approval and consent to participate
Ethical approval for the study was granted by the Institutional Experimental Animal Care and Use Committee of the Ministry of Agriculture and Rural Affairs of China and the Animal Care and Use Committee at China Agricultural University (AW01103202-1–31, AW72104202-1–2).

Consent for publication
Not applicable.

Competing interests
The authors declare no competing interests.

Author details
[1]State Key Laboratory of Animal Nutrition and Feeding, Department of Animal Nutrition and Feed Science, College of Animal Science and Technology, China Agricultural University, Beijing 100193, China. [2]Laboratory of Animal Neurobiology, College of Veterinary Medicine, Nanjing Agricultural University, Nanjing 210095, China. [3]College of Animal Science, Xinjiang Agricultural University, Urumqi 830052, China. [4]College of Animal Science and Technology, Ningxia University, Yinchuan 750021, China. [5]Key Laboratory for Dairy Cow Nutrition, Institute of Feed Research of Chinese Academy of Agricultural Sciences, Beijing 100081, China.

Received: 12 June 2024 Accepted: 4 February 2025
Published online: 08 March 2025

References

1. Hannan FM, Elajnaf T, Vandenberg LN, Kennedy SH, Thakker RV. Hormonal regulation of mammary gland development and lactation. Nat Rev Endocrinol. 2023;19:46–61.
2. Ghaffari MH, Sadri H, Sauerwein H. Invited review: assessment of body condition score and body fat reserves in relation to insulin sensitivity and metabolic phenotyping in dairy cows. J Dairy Sci. 2023;106:807–21.
3. Kovacs CS. Maternal mineral and bone metabolism during pregnancy, lactation, and post-weaning recovery. Physiol Rev. 2016;96:449–547.
4. Miglior F, Fleming A, Malchiodi F, Brito LF, Martin P, Baes CF. A 100-year review: identification and genetic selection of economically important traits in dairy cattle. J Dairy Sci. 2017;100:10251–71.
5. LeBlanc S. Monitoring metabolic health of dairy cattle in the transition period. J Reprod Dev. 2010;56(Suppl):S29-35.
6. Cainzos JM, Andreu-Vazquez C, Guadagnini M, Rijpert-Duvivier A, Duffield T. A systematic review of the cost of ketosis in dairy cattle. J Dairy Sci. 2022;105:6175–95.
7. De Vries A. Symposium review: why revisit dairy cattle productive lifespan? J Dairy Sci. 2020;103:3838–45.
8. Zachos FE. Walker's mammals of the world. Monotremes, marsupials, afrotherians, xenarthrans, and sundatherians. Baltimore: Johns Hopkins University Press; 2019.
9. Andersson L. Subclinical ketosis in dairy cows. Vet Clin N Am-Food A. 1988;4:233–51.
10. McArt JAA, Nydam DV, Overton MW. Hyperketonemia in early lactation dairy cattle: a deterministic estimate of component and total cost per case. J Dairy Sci. 2015;98:2043–54.
11. Rodriguez Z, Shepley E, Endres MI, Cramer G, Caixeta LS. Assessment of milk yield and composition, early reproductive performance, and herd removal in multiparous dairy cattle based on the week of diagnosis of hyperketonemia in early lactation. J Dairy Sci. 2022;105:4410–20.
12. Raboisson D, Mounie M, Maigne E. Diseases, reproductive performance, and changes in milk production associated with subclinical ketosis in dairy cows: a meta-analysis and review. J Dairy Sci. 2014;97:7547–63.
13. McArt JAA, Nydam DV, Oetzel GR. Epidemiology of subclinical ketosis in early lactation dairy cattle. J Dairy Sci. 2012;95:5056–66.
14. Halfen J, Carpinelli NA, Lasso-Ramirez S, Michelotti TC, Fowler EC, St-Pierre B, et al. Physiological conditions leading to maternal subclinical ketosis in holstein dairy cows can impair the offspring's postnatal growth and gut microbiome development. Microorganisms. 2023;11:1839.
15. Reynolds CK, Huntington GB, Tyrrell HF, Reynolds PJ. Net metabolism of volatile fatty acids, d-beta-hydroxybutyrate, nonesterifield fatty acids, and blood gasses by portal-drained viscera and liver of lactating holstein cows. J Dairy Sci. 1988;71:2395–405.
16. Zhang J, Gaowa N, Wang Y, Li H, Cao Z, Yang H, et al. Complementary hepatic metabolomics and proteomics reveal the adaptive mechanisms of dairy cows to the transition period. J Dairy Sci. 2023;106:2071–88.
17. Gonzalez-Garcia R, McCubbin T, Navone L, Stowers C, Nielsen L, Marcellin E. Microbial propionic acid production. Fermentation. 2017;3:21.
18. Reichardt N, Duncan SH, Young P, Belenguer A, McWilliam Leitch C, Scott KP, et al. Phylogenetic distribution of three pathways for propionate production within the human gut microbiota. ISME J. 2014;8:1323–35.
19. Derakhshani H, Tun HM, Cardoso FC, Plaizier JC, Khafipour E, Loor JJ. Linking peripartal dynamics of ruminal microbiota to dietary changes and production parameters. Front Microbiol. 2016;7:2143.
20. Zhu Z, Kristensen L, Difford GF, Poulsen M, Noel SJ, Abu Al-Soud W, et al. Changes in rumen bacterial and archaeal communities over the transition period in primiparous holstein dairy cows. J Dairy Sci. 2018;101:9847–62.
21. Kong F, Wang F, Zhang Y, Wang S, Wang W, Li S. Repeated inoculation with rumen fluid accelerates the rumen bacterial transition with no

benefit on production performance in postpartum holstein dairy cows. J Anim Sci Biotechnol. 2024;15:17.
22. Gebreyesus G, Difford GF, Buitenhuis B, Lassen J, Noel SJ, Hojberg O, et al. Predictive ability of host genetics and rumen microbiome for subclinical ketosis. J Dairy Sci. 2020;103:4557–69.
23. Wang X, Li X, Zhao C, Hu P, Chen H, Liu Z, et al. Correlation between composition of the bacterial community and concentration of volatile fatty acids in the rumen during the transition period and ketosis in dairy cows. Appl Environ Microbiol. 2012;78:2386–92.
24. Wang Q, Cui Y, Indugu N, Loor JJ, Jiang Q, Yu Z, et al. Integrated meta-omics analyses reveal a role of ruminal microorganisms in ketone body accumulation and ketosis in lactating dairy cows. J Dairy Sci. 2023;106:4906–17.
25. Bach A, López-García A, González-Recio O, Elcoso G, Fàbregas F, Chaucheyras-Durand F, et al. Changes in the rumen and colon microbiota and effects of live yeast dietary supplementation during the transition from the dry period to lactation of dairy cows. J Dairy Sci. 2019;102:6180–98.
26. Pitta DW, Kumar S, Vecchiarelli B, Shirley DJ, Bittinger K, Baker LD, et al. Temporal dynamics in the ruminal microbiome of dairy cows during the transition period. J Anim Sci. 2014;92:4014–22.
27. Luo Z, Du Z, Huang Y, Zhou T, Wu D, Yao X, et al. Alterations in the gut microbiota and its metabolites contribute to metabolic maladaptation in dairy cows during the development of hyperketonemia. mSystems. 2024;9:e0002324.
28. Allaband C, Lingaraju A, Flores Ramos S, Kumar T, Javaheri H, Tiu MD, et al. Time of sample collection is critical for the replicability of microbiome analyses. Nat Metab. 2024;6:1282–93.
29. McCarthy MM, Mann S, Nydam DV, Overton TR, McArt JA. Short communication: concentrations of nonesterified fatty acids and beta-hydroxybutyrate in dairy cows are not well correlated during the transition period. J Dairy Sci. 2015;98:6284–90.
30. Kaufman EI, Asselstine VH, LeBlanc SJ, Duffield TF, DeVries TJ. Association of rumination time and health status with milk yield and composition in early-lactation dairy cows. J Dairy Sci. 2018;101:462–71.
31. O'Hara E, Neves ALA, Song Y, Guan LL. The role of the gut microbiome in cattle production and health: driver or passenger? Annu Rev Anim Biosci. 2020;8:199–220.
32. National research council. Nutrient requirements of dairy cattle: seventh revised edition, 2001. Washington, DC: The National Academies Press; 2001.
33. Rodriguez Z, Caixeta LS, Cramer G. Diagnostic accuracy of a bovine specific electronic beta-hydroxybutyrate handheld meter in fresh blood and stored serum samples. Vet Anim Sci. 2021;11:100159.
34. Edmonson AJ, Lean IJ, Weaver LD, Farver T, Webster G. A body condition scoring chart for holstein dairy cows. J Dairy Sci. 1989;72:68–78.
35. Kong F, Gao Y, Tang M, Fu T, Diao Q, Bi Y, et al. Effects of dietary rumen-protected lys levels on rumen fermentation and bacterial community composition in holstein heifers. Appl Microbiol Biotechnol. 2020;104:6623–34.
36. Toledo MZ, Nienow C, Luchini D, Arriola Apelo SI, Wiltbank MC. Quantification of bovine plasma amino acids via liquid chromatography–electrospray ionization-mass spectrometry: comparison of underivatized and precolumn derivatized methods. JDS Commun. 2021;2:227–32.
37. Wang D, Chen L, Tang G, Yu J, Chen J, Li Z, et al. Multi-omics revealed the long-term effect of ruminal keystone bacteria and the microbial metabolome on lactation performance in adult dairy goats. Microbiome. 2023;11:215.
38. Bolyen E, Rideout JR, Dillon MR, Bokulich NA, Abnet CC, Al-Ghalith GA, et al. Author correction: reproducible, interactive, scalable and extensible microbiome data science using qiime 2. Nat Biotechnol. 2019;37:1091.
39. Kechin A, Boyarskikh U, Kel A, Filipenko M. Cutprimers: a new tool for accurate cutting of primers from reads of targeted next generation sequencing. J Comput Biol. 2017;24:1138–43.
40. Callahan BJ, McMurdie PJ, Rosen MJ, Han AW, Johnson AJ, Holmes SP. Dada2: high-resolution sample inference from illumina amplicon data. Nat Methods. 2016;13:581–3.
41. Katoh K, Misawa K, Kuma K, Miyata T. MAFFT: a novel method for rapid multiple sequence alignment based on fast fourier transform. Nucleic Acids Res. 2002;30:3059–66.
42. Quast C, Pruesse E, Yilmaz P, Gerken J, Schweer T, Yarza P, et al. The silva ribosomal rna gene database project: improved data processing and web-based tools. Nucleic Acids Res. 2013;41:D590–6.
43. Adebayo Arowolo M, Zhang XM, Wang M, Wang R, Wen JN, Hao LZ, et al. Proper motility enhances rumen fermentation and microbial protein synthesis with decreased saturation of dissolved gases in rumen simulation technique. J Dairy Sci. 2022;105:231–41.
44. Stevenson DM, Weimer PJ. Dominance of prevotella and low abundance of classical ruminal bacterial species in the bovine rumen revealed by relative quantification real-time pcr. Appl Microbiol Biotechnol. 2007;75:165–74.
45. Sylvester JT, Karnati SKR, Yu Z, Morrison M, Firkins JL. Development of an assay to quantify rumen ciliate protozoal biomass in cows using real-time pcr. J Nutr. 2004;134:3378–84.
46. Zhou M, Hernandez-Sanabria E, Guan LL. Assessment of the microbial ecology of ruminal methanogens in cattle with different feed efficiencies. Appl Environ Microb. 2009;75:6524–33.
47. Denman SE, McSweeney CS. Development of a real-time pcr assay for monitoring anaerobic fungal and cellulolytic bacterial populations within the rumen. Fems Microbiol Ecol. 2006;58:572–82.
48. Martin M. Cutadapt removes adapter sequences from high-throughput sequencing reads. EMBnet J. 2011;17:10–2.
49. Chen S, Zhou Y, Chen Y, Gu J. Fastp: an ultra-fast all-in-one fastq preprocessor. Bioinformatics. 2018;34:i884–90.
50. Li H. Minimap2: Pairwise alignment for nucleotide sequences. Bioinformatics. 2018;34:3094–100.
51. Menzel P, Ng KL, Krogh A. Fast and sensitive taxonomic classification for metagenomics with kaiju. Nat Commun. 2016;7:11257.
52. Li D, Liu CM, Luo R, Sadakane K, Lam TW. MEGAHIT: an ultra-fast single-node solution for large and complex metagenomics assembly via succinct de Bruijn graph. Bioinformatics. 2015;31:1674–6.
53. Steinegger M, Söding J. Mmseqs2 enables sensitive protein sequence searching for the analysis of massive data sets. Nat Biotechnol. 2017;35:1026–8.
54. Hyatt D, Chen GL, Locascio PF, Land ML, Larimer FW, Hauser LJ. Prodigal: prokaryotic gene recognition and translation initiation site identification. BMC Bioinformatics. 2010;11:119.
55. Liao Y, Smyth GK, Shi W. featureCounts: an efficient general purpose program for assigning sequence reads to genomic features. Bioinformatics. 2014;30:923–30.
56. Bu D, Luo H, Huo P, Wang Z, Zhang S, He Z, et al. KOBAS-i: intelligent prioritization and exploratory visualization of biological functions for gene enrichment analysis. Nucleic Acids Res. 2021;49:W317–25.
57. Holmes I, Harris K, Quince C. Dirichlet multinomial mixtures: generative models for microbial metagenomics. PLoS ONE. 2012;7:e30126.
58. Stewart CJ, Ajami NJ, O'Brien JL, Hutchinson DS, Smith DP, Wong MC, et al. Temporal development of the gut microbiome in early childhood from the teddy study. Nature. 2018;562:583–8.
59. DiGiulio DB, Callahan BJ, McMurdie PJ, Costello EK, Lyell DJ, Robaczewska A, et al. Temporal and spatial variation of the human microbiota during pregnancy. P Natl Acad Sci USA. 2015;112:11060–5.
60. Baron RM, Kenny DA. The moderator-mediator variable distinction in social psychological research: conceptual, strategic, and statistical considerations. J Pers Soc Psychol. 1986;51:1173–82.
61. Daniel J-B, Sanz-Fernandez MV, Nichols K, Doelman J, Martín-Tereso J. Digestive and metabolic efficiency of energy and nitrogen during lactation and the dry period in dairy cows. J Dairy Sci. 2022;105:9564–80.
62. Kessel S, Stroehl M, Meyer HH, Hiss S, Sauerwein H, Schwarz FJ, et al. Individual variability in physiological adaptation to metabolic stress during early lactation in dairy cows kept under equal conditions. J Anim Sci. 2008;86:2903–12.
63. Huang Y, Zhang B, Mauck J, Loor JJ, Wei B, Shen B, et al. Plasma and milk metabolomics profiles in dairy cows with subclinical and clinical ketosis. J Dairy Sci. 2024;107:6340–57.
64. Eom JS, Kim HS, Lee SJ, Choi YY, Jo SU, Kim J, et al. Metabolic profiling of rumen fluid and milk in lactating dairy cattle influenced by subclinical ketosis using proton nuclear magnetic resonance spectroscopy. Animals (Basel). 2021;11:2526.
65. Zhao C, Hu X, Bao L, Wu K, Zhao Y, Xiang K, et al. Gut dysbiosis induces the development of mastitis through a reduction in host anti-inflammatory enzyme activity by endotoxemia. Microbiome. 2022;10:205.
66. Krizsan SJ, Ahvenjärvi S, Huhtanen P. A meta-analysis of passage rate estimated by rumen evacuation with cattle and evaluation of passage rate prediction models. J Dairy Sci. 2010;93:5890–901.
67. Shabat SK, Sasson G, Doron-Faigenboim A, Durman T, Yaacoby S, Berg Miller ME, et al. Specific microbiome-dependent mechanisms underlie the energy harvest efficiency of ruminants. ISME J. 2016;10:2958–72.

68. Xiang K, Li S, Tuniyazi M, Mu R, Wang Y, Zhang N, et al. Changes in the rumen microbiota community in ketosis cows during propylene glycol treatment. Food Funct. 2022;13:7144–56.
69. Vieira-Silva S, Falony G, Darzi Y, Lima-Mendez G, Garcia Yunta R, Okuda S, et al. Species–function relationships shape ecological properties of the human gut microbiome. Nat Microbiol. 2016;1:16088.
70. Hasin Y, Seldin M, Lusis A. Multi-omics approaches to disease. Genome Biol. 2017;18:83.
71. Liu P, Liu Y, Cheng J, Xia Y, Yang Y. Copper exposure causes alteration in the intestinal microbiota and metabolites in takifugu rubripes. Ecotox Environ Safe. 2024;272:116064.
72. Zhang W, Xu X, Cai L, Cai X. Dysbiosis of the gut microbiome in elderly patients with hepatocellular carcinoma. Sci Rep. 2023;13:7797.
73. Betancur-Murillo CL, Aguilar-Marín SB, Jovel J. Prevotella: a key player in ruminal metabolism. Microorganisms. 2022;11:1.
74. Kovatcheva-Datchary P, Nilsson A, Akrami R, Lee Ying S, De Vadder F, Arora T, et al. Dietary fiber-induced improvement in glucose metabolism is associated with increased abundance of prevotella. Cell Metab. 2015;22:971–82.
75. La Reau AJ, Suen G. The ruminococci: key symbionts of the gut ecosystem. J Microbiol. 2018;56:199–208.
76. Wylensek D, Hitch TCA, Riedel T, Afrizal A, Kumar N, Wortmann E, et al. A collection of bacterial isolates from the pig intestine reveals functional and taxonomic diversity. Nat Commun. 2020;11:6389.
77. Gaffney J, Embree J, Gilmore S, Embree M. Chordicoccus furentiruminis, gen. nov., sp. nov., a novel succinic acid producing bacterium isolated from a steer on a high grain diet. Int J Syst Evol Micr. 2023;73:005751.
78. Schmidt GH, Schultz LH. Effect of feeding sodium propionate on milk and fat production, roughage consumption, blood sugar, and blood ketones of dairy cows1. J Dairy Sci. 1958;41:169–75.
79. Oba M, Allen MS. Dose-response effects of intrauminal infusion of propionate on feeding behavior of lactating cows in early or midlactation. J Dairy Sci. 2003;86:2922–31.
80. Albornoz RI, Allen MS. Highly fermentable starch at different diet starch concentrations decreased feed intake and milk yield of cows in the early postpartum period. J Dairy Sci. 2018;101:8902–15.
81. Hristov AN, Bannink A, Crompton LA, Huhtanen P, Kreuzer M, McGee M, et al. Invited review: nitrogen in ruminant nutrition: a review of measurement techniques. J Dairy Sci. 2019;102:5811–52.
82. Baumgard LH, Collier RJ, Bauman DE. A 100-year review: regulation of nutrient partitioning to support lactation. J Dairy Sci. 2017;100:10353–66.
83. Rulquin H, Rigout S, Lemosquet S, Bach A. Infusion of glucose directs circulating amino acids to the mammary gland in well-fed dairy cows. J Dairy Sci. 2004;87:340–9.
84. Whitehouse NL, Schwab CG, Brito AF. The plasma free amino acid dose-response technique: a proposed methodology for determining lysine relative bioavailability of rumen-protected lysine supplements. J Dairy Sci. 2017;100:9585–601.
85. Fetter ME, Cunningham DM, Gambonini F, Räisänen SE, Ott TL, Hristov AN. Short communication: postpartum plasma amino acid concentration in primi- and multiparous Holstein cows. Anim Feed Sci Tech. 2021;281:115101.
86. Wang Y, Gao Y, Xia C, Zhang H, Qian W, Cao Y. Pathway analysis of plasma different metabolites for dairy cow ketosis. Ital J Anim Sci. 2016;15:545–51.
87. Weber C, Losand B, Tuchscherer A, Rehbock F, Blum E, Yang W, et al. Effects of dry period length on milk production, body condition, metabolites, and hepatic glucose metabolism in dairy cows. J Dairy Sci. 2015;98:1772–85.
88. Kao CC, Cope JL, Hsu JW, Dwarkanath P, Karnes JM, Luna RA, et al. The microbiome, intestinal function, and arginine metabolism of healthy Indian women are different from those of American and Jamaican women. J Nutr. 2016;146:706–13.
89. Jo S, Kang W, Hwang YS, Lee SH, Park KW, Kim MS, et al. Oral and gut dysbiosis leads to functional alterations in Parkinson's disease. NPJ Parkinsons Dis. 2022;8:87.

Publisher's Note